

Report on the
Power Output of a Solid Pellet Water
Bath Calorimeter,
Light Power Output of a Solid Pellet,
and SunCell® Output Power
at Brilliant Light Power

by

Randy A. Booker

Randy Booker, Ph.D.
Department of Physics
UNC Asheville
May 31, 2016

This report outlines results I validated for four types of experiments when I visited Brilliant Light Power of Cranbury, New Jersey, on May 23-24, 2016. I was able to validate 1) the measurements for the energy input and energy output of a single-initiation solid pellet using a commercial water bath calorimeter, 2) single-initiation solid fuel pellet light output by measuring the power output using absolute spectroscopy with two types of fuels and spectroscopic approaches for peak power and average power, and 3) the thermal coolant temperature response to the activation of the hydrino reaction in the continuous power cell known as the SunCell.

Of main importance to validate in these experiments were: the procedure used for carrying out the experiment, that the experiment was carried out correctly in front of an impartial validator (myself), and the measurement of the excess power output in each of these four types of experiments.

I. Power Output of a Solid Pellet Water Bath Calorimeter

A 2 mm diameter hydrated silver shot that served as a source of oxygen inside it and an argon-hydrogen (95/5%) atmosphere that served as a source of atomic hydrogen formed a hydrino HOH-based solid fuel when the shot was ignited by applying a current of about 20,000 A through the fuel. The fuel was held between two electrodes of a low-voltage, high current power source that applied the current. This apparatus was then placed inside the cell of a commercial bomb calorimeter, a PARR 1341 water bath calorimeter. The energy released from a 10 microliter shot of about 80 mg by the nascent HOH (not hydrogen bonded in solid, liquid, or gaseous state) catalyzed transition of H to hydrino state $H_2(1/4)$ was observed to be up to 171 J for a 0.7 ms ignition event corresponding to an average power of 244,000 W.

More detail on the theory behind this experiment and detailed diagrams of the apparatus can be found in Appendix A.

The shots were formed by melting silver and in a graphite crucible. These approximately 80 mg shots contained 1 mol% . The shot contained about 1% mole water content as determined by X-ray diffraction (XRD). To serve as a calibration of this system, cylindrical copper caps served as the control in order to determine the heat capacity of the calorimeter. Also chromium metal flakes of thickness 2 mm were used as a control that melted and produced an arc plasma. For the control cases, the cell gas was Argon. For the non-control cases, the cell gas was 95% argon and 5% hydrogen at one atmosphere of pressure.

Each oxide-doped silver shot having a resistance of about 150 uohms was ignited with a peak current of about 20,000 A yielding a shot voltage drop of about 3 V and a peak ignition power of under 75,000 W from a 75 KVA current source. The input power waveform was determined by multiplying the measured voltage waveform (given by the voltage taps immediately above the water level) with the measured current waveform given by the Rogowski coil . This power waveform was time integrated to yield the cumulative energy input.



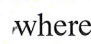
During the running of the actual experiments, I was allowed to observe the entire experiment from the loading of the cell into the calorimeter, to placing the silver shot between the electrodes,

to taking the data, and to asking questions about the procedure and the data taking. I was able to inspect the silver pellets between the electrodes before and after the experiments.


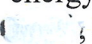
Using the copper metal caps in Table 1, the heat capacity of the calorimeter and electrode apparatus used to measure the energy balance of solid fuel samples was found to be 6400 J/°C. As seen in Table 1, almost zero net energy balance was measured on both experiments using the control Chromium foil flakes. The Power Fitted Energy Net = Thermal Energy Out – Power Fitted Energy Input is found to be 2.6 J and 4.5 J, respectively.

Table 1. Determination of the energy balance of the hydrino solid fuel by bomb calorimetry.

Experiment and Description	Purpose	Purge	VI Energy Input (J)	VI Power Fitted Energy Input (J)	Room Temp @ Fire Time (°C)	Event Duration (End-Fire time) (min)	Total dT (°C)	Parr Calc'd dT (°C)	Pre Slope (°C/min)	Post Slope (°C/min)	Thermal Energy Out (J)	VI Power Fitted Energy Input (J)	VI Power Fitted Energy Gain (J)	VI Power Fitted Energy Net (J)	VI Energy Input (J)	VI Energy Gain (J)	VI Energy Net (J)
2016-05-24-MY4 Cr flake control 77.9 mg (~2.8 x 3.0 x 2.3 mm), 55 lbs.	Testing disruptive control	5min UHP Ar	284.0	256.6	23.84	4.22	0.0340	0.0405	-0.002293	-0.001454	259.3	256.6	1.01	2.6	284.0	0.91	-24.7
2016-05-24-MY3 Ag ⁺ (1 mol%) pellet, 76.4 mg, 175 lbs.	Testing batch 051716RF2 Ag ⁺ (1 mol%) pellet	5min 5% H ₂ :Ar	377.7	230.6	23.59	5.98	0.0530	0.0606	-0.001821	-0.001095	387.9	230.6	1.68	157.3	377.7	1.03	10.2
2016-05-24-MY1 Ag ⁺ (1 mol%) pellet, 75.0 mg, 175 lbs.	Testing batch 040816CC1 Ag ⁺ (1 mol%) pellet	5min 5% H ₂ :Ar	368.5	196.6	23.05	5.60	0.0520	0.0574	-0.001633	-0.000821	367.6	196.6	1.87	171.0	368.5	1.00	-0.9
2016-05-23-MY3 Cr flake control 81.0 mg (~2.9x2.6 x 2.1 mm), 55 lbs.	Testing disruptive control	5min UHP Ar	270.0	234.5	23.54	7.10	0.0300	0.0374	-0.001589	-0.000833	239.1	234.5	1.02	4.5	270.0	0.89	-30.9
2016-05-23-MY2 Ag ⁺ (1 mol%) pellet, 75.0 mg, 175 lbs.	Testing batch 040816CC1 Ag ⁺ (1 mol%) pellet	5min 5% H ₂ :Ar	376.5	208.1	23.35	6.88	0.0520	0.0587	-0.001893	-0.000748	375.5	208.1	1.80	167.4	376.5	1.00	-1.0
2016-05-23-MY1 Cu Caps control, 175 lbs.	Testing resistive control	5min UHP Ar	248.4	248.4	23.03	5.85	0.0360	0.0412	-0.001556	-0.000654	263.6	248.4	1.06	15.2	248.4	1.06	15.2

Contrasted with the near zero energy balance, significant energies and powers were observed for the silver pellets where HOH served as a catalyst for a hydrino transition, with the subsequent release of significant energy. The net energies observed were 157.3 J using Ag +  171.0 J using Ag +  and 167.4 J for Ag⁺  wherein all were run in an Ar/H₂ atmosphere. Since the ignition time was on the order of 0.7 ms, these energies correspond to 225,000 W, 244,000 W, and 239,000 W, respectively. This is a tremendous amount of power generated from these small solid pellets of silver, each of about 10 ul volume.

Executive Summary

Brilliant Light Power has discovered a novel new heat source, which produces a large excess of heat. These output power numbers have been validated by me, and are correct. I have been given access to the data files taken during the experiments for this validation. Also, for ; no known reaction exists for energy to be generated since there's no known energy-releasing reaction involving silver, , argon, and hydrogen. All the observed energy in these cases must come from the arc discharge of the pellet itself. I am led to the conclusion that the generation of the net excess heat in the solid fuel reaction cell experiment is real and reproducible.

II. Light Power Output of a Solid Pellet

Hydrated silver shots were ignited by passing a low voltage (less than 6V) yet high current (~23,000-25,000 A) through the shot which produced an explosive plasma that emitted bright light occurring mostly in the EUV to UV range of 10-300 nm. The source of the light was due to the HOH catalyzed transition of H to the lower energy hydrino state $H(1/4)$, caused by the arc current producing a nascent HOH and H plasma. The power and bright light released from the ignition of this silver pellet were determined by using absolute spectroscopy over the 22.8-647 nm region. The radiation produced occurred in the EUV and UV range with almost no light occurring in the visible or infrared.

More detail on the theory behind this experiment and detailed diagrams of the apparatus can be found in Appendix B.

Before taking spectra of the ignited silver shots, the spectrometer slit width was measured using the diffraction pattern from a helium-neon laser, the spectrometer was wavelength calibrated using 4 bright spectral lines from a mercury source, and absolute irradiance was calibrated using a NIST traceable calibrated tungsten-filament light bulb that was slowly powered on to its specified operating calibration current. I was on-hand during these calibrations and they were done cautiously and carefully. Then the spectrometer was used to detect the bright light coming off the ignitions of several silver shots.

I was on-hand when the spectra were being taken and I observed the data taking. I was able to inspect the silver pellets between the electrodes before and after the experiments. I was able to inspect the mounting of the pellets in the reaction vessel. And I was able to ask questions about the procedure and the data taking as they were on going. I also have been given access to the data tables taken during these experiments. These output power numbers have been validated by me, and are correct.

Figures 1-4 show the spectra we took during our runs. In Figure 1, you see the raw data where we first ran the spectrum centered on 200 nm, next we ran a spectrum centered on 300 nm, then we ran a spectrum centered on 400 nm, and lastly a spectrum centered on 500 nm. These all used the McPherson normal incidence spectrometer using an MgF_2 window. Next spectra were taken centered at 100 nm and 200 nm using the same spectrometer without a window. Lastly a spectrum was taken using the McPherson grazing incidence spectrometer centered on 55 nm using an Al filter. These produced Figures 1-3 with the appropriate calibrated instrument corrections and conversion to power. The EUV spectrum was matched to the absolute calibrated UV-Vis Mightex spectrum in the region of spectral overlap to give the full power spectrum shown in Figure 4.

Figure 1. The raw spectra obtained using the GIS and NIS spectrometer to be processed with window, filter, grating, and CCD quantum efficiency corrections.

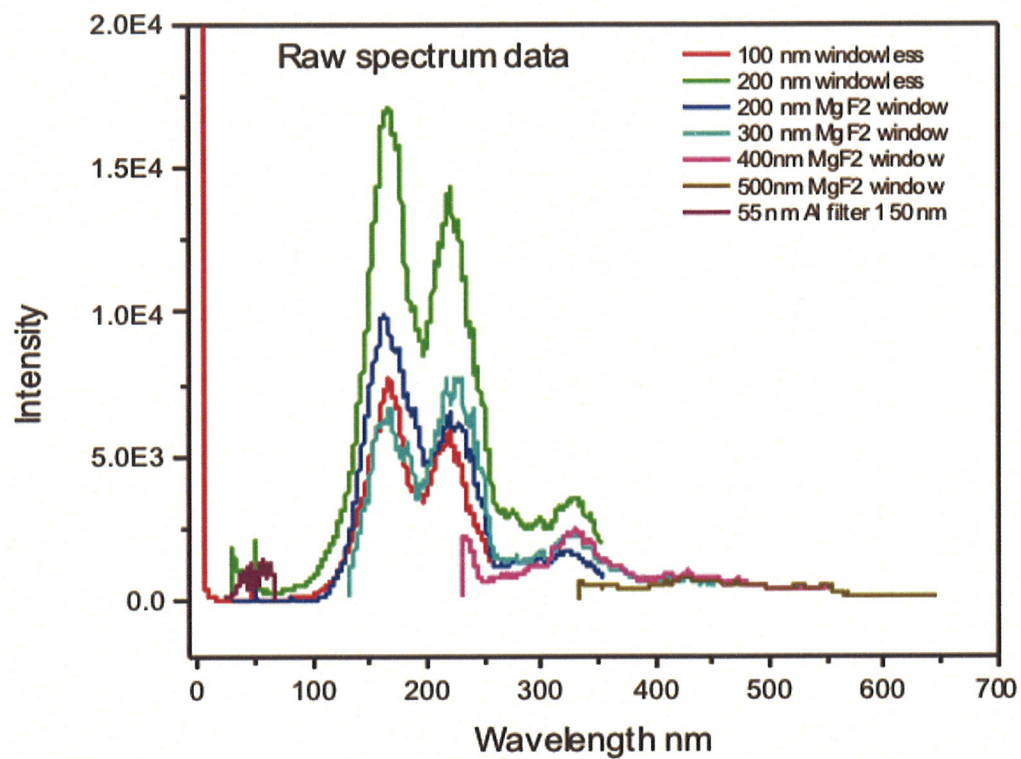


Figure 2. The combined GIS and NIS spectra following filter, grating, and CCD quantum efficiency corrections.

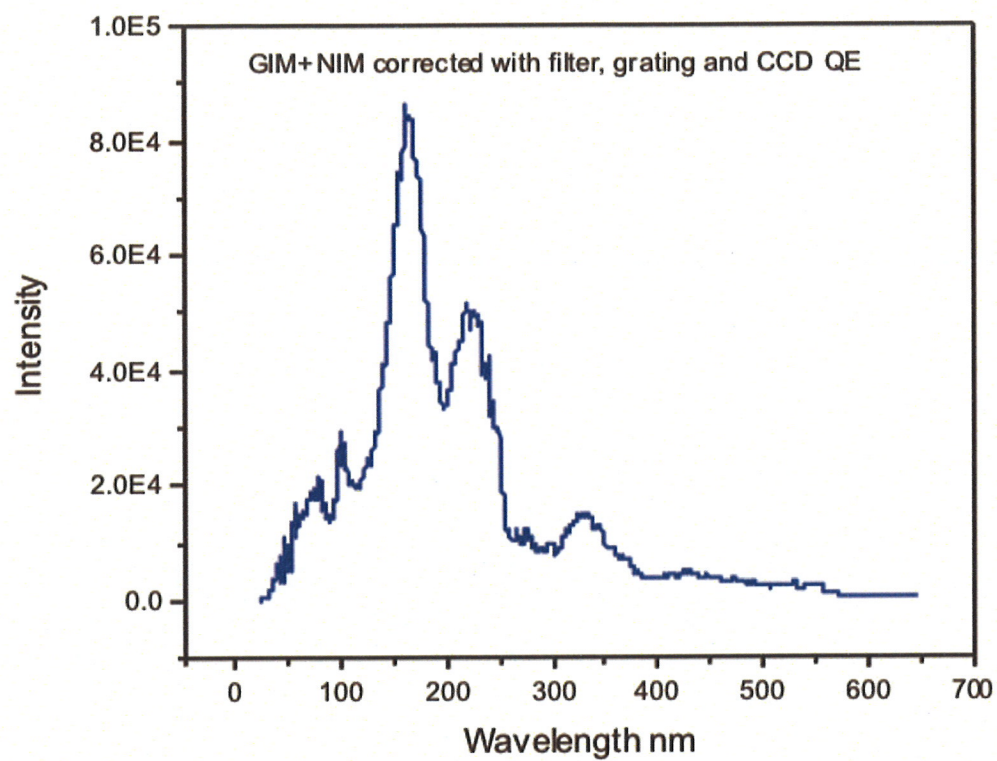


Figure 3. The combined GIS and NIS spectra before power calibration against the absolutely calibrated UV-Vis spectrum wherein the spectral count intensity of Fig. 2 was converted to energy density by multiplying the counts as a function of wavelength by $\frac{hc}{\lambda}$.

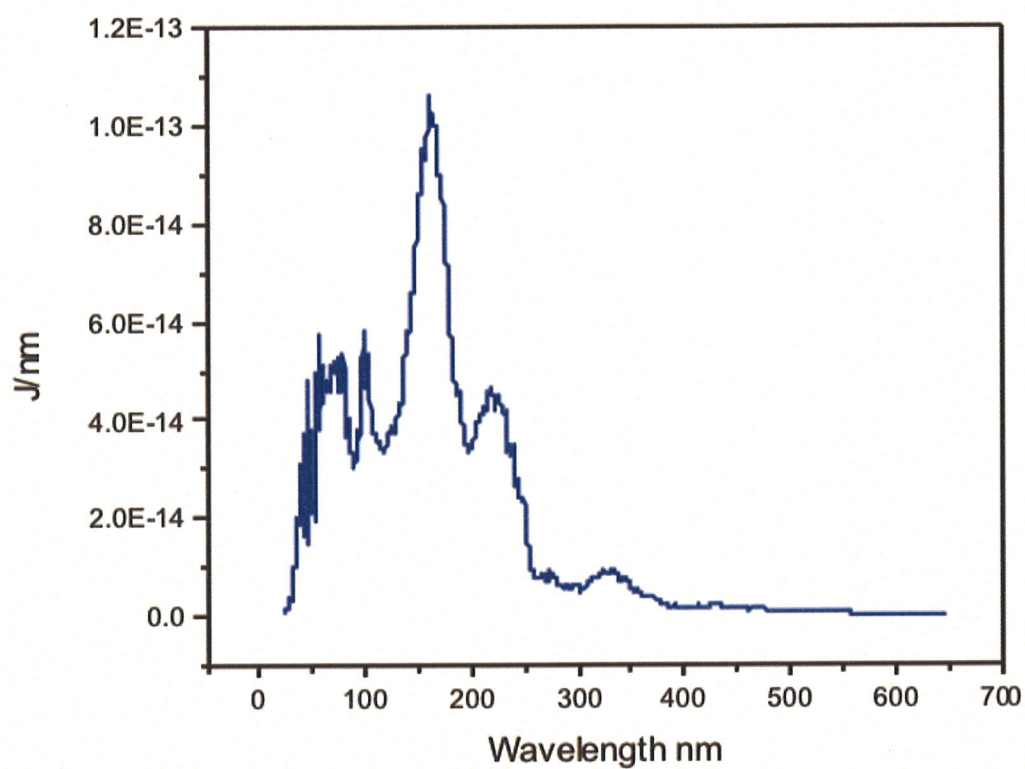
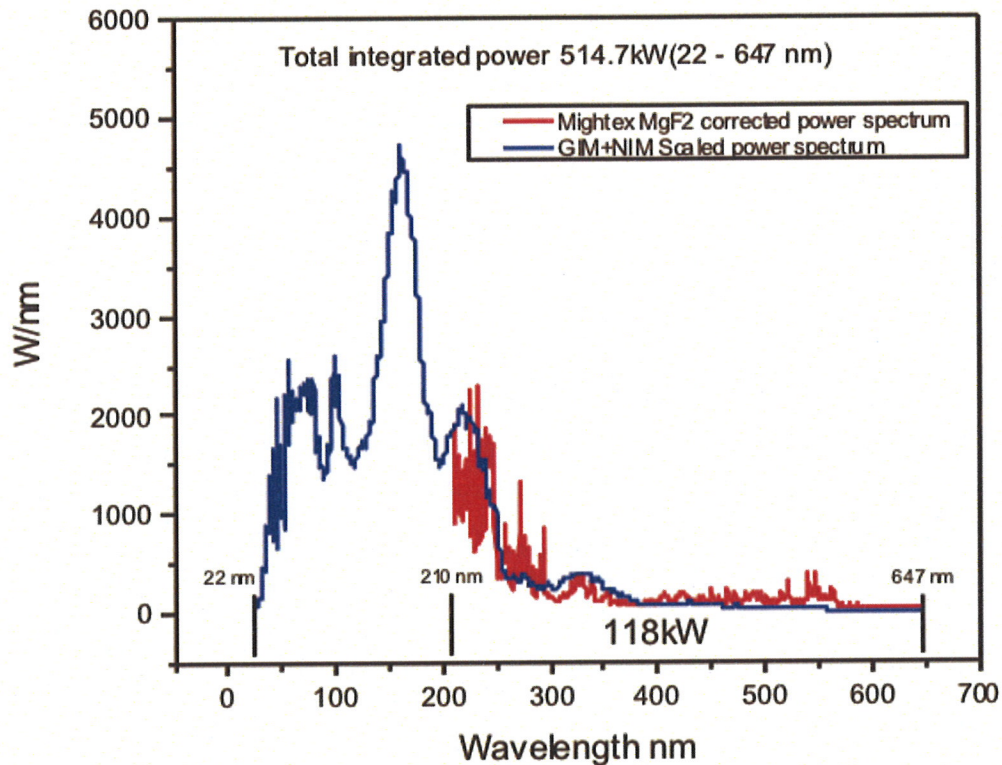




Figure 4. The wavelength calibrated and absolute intensity calibrated spectrum (22.8-647 nm) of the emission of hydrated silver shots comprising a source of H and HOH hydrino catalyst that were ignited by passing a low voltage, high current through the shot. The radiation is predominantly in the high-energy region with the predicted short wavelength emission of the H(1/4) continuum radiation.




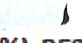

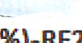



From Figure 4, the representative power of ignited silver shot in the region of 22 to 647 nm was 514.7 kW. This corresponded to 350 J of energy in a 0.68 ms blast ignition event. Using fast time resolved spectroscopy, the peak light power was determined to be 2.1 MW corresponding to 83.6 J of energy generated in 40 microseconds. The power is remarkable considering that the source was a silver shot of only about 10 microliter volume. The 2.1 MW of optical power also significantly exceeded the power rating of the ignition source, 75 KVA.

In addition to hydrated silver pellets, silver shots impregnated with a very stable metal as a source of oxygen were ignited, and the peak power and energy in the ultraviolet range was recorded at fast time resolution. As seen in Table 2, the peak power generated from the ignition of doped silver pellets in vacuum were in the range of 382-689.4 kW as determined using 40 μ s time resolved spectroscopy with the absolute irradiance calibrated Mightex spectrometer

(200-816 nm). From the full spectrum (Figure 4), the total optical power of the 22.8-647 nm region was shown to be about 4.1 times the optical power in the UV (> 200 nm) range; so the total peak optical power was much higher, greater than 2.8 MW. The hydrino reaction requires atomic hydrogen that is supported in plasma comprising low concentrations of hydrogen in an inert gas such as argon; whereas, atmospheric pressure hydrogen plasma comprises predominantly unreactive molecular hydrogen. As seen from the first two runs of Table 2, the power produced by ignition of the oxide-doped shots in a pure H₂ atmosphere was reduced by about a factor of five, 176 kW and 94.8 kW. The pure hydrogen gas suppressed hydrino reactions and thereby reduced the power output, as expected.


Table 2. The results of the absolute spectroscopy recorded on ignited hydrated silver shots, at least partially dehydrated silver shots, and partially hydrated 80-90 mg silver- (3 mole%) and silver- (1-3 mole%) shots over the range of 200-816 nm.

Setup Atm	Sample Type	Sample Mass (mg)	Peak Waveform Current (kA)	Mightex Energy (J)	Mightex Max Power (kW)
H2	Ag-  (3mol%)-RF1	85.0	22.9	28.4	176.0
H2	Ag+  (3mol%)-RF2	82.0	22.1	16.8	94.8
Vacuum	Ag-  (3mol%)-RF0	87.0	22.2	92.0	382.0
Vacuum	Ag-  (3mol%)-RF2	88.0	23.8	88.0	385.9
Vacuum	Ag+  (3mol%)-RF2	82.4	24.4	141.2	567.7
Vacuum	Ag+  (1mol%)-RF2	82.3	21.8	101.3	485.1
Vacuum	Ag+  (1mol%)-RF2	81.1	23.7	138.3	689.4

Executive Summary

Brilliant Light Power has discovered a novel new power source, which produces a large excess of power and light. These output power numbers have been validated by me, and are correct. I have been given access to the data files for analysis, and I am led to the conclusion that the generation of the net excess power and light in the solid fuel reaction cell experiment is real and reproducible.

III. SunCell® Output Power

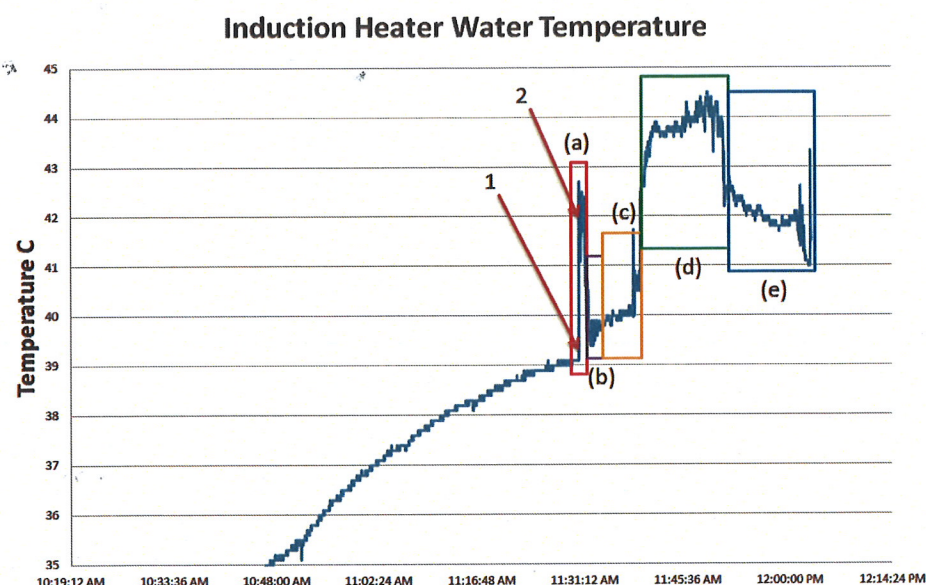
The SunCell® utilized to produce high hydrino reaction power generates an arc current plasma by low plasma voltage (<5 V), high current (~5 kA) pulses through highly conducting molten silver impregnated with trace amounts of a stable metal  that is injected between two tungsten electrodes in the presence of flowing hydrogen mixed in argon. These electrodes provide the plasma-initiating electric pulses for the reaction at a frequency of about 0.5 to 1 kHz

to achieve essentially constant plasma ignition. This ignition system is made up of three pairs of three capacitors in series attached to the tungsten electrodes. Following ignition, the molten metal returns downward to the injection system by gravity flow. The hydride reactants of atomic H and nascent HOH catalyst are formed in the plasma from supplied 3% hydrogen gas in argon flowed at 9 liters per min corresponding to about 2×10^{-4} moles H_2/s wherein one mole% H_2 or 0.5 mole% H_2O supplies O for the HOH catalyst. The SunCell[®] is made of four fundamental systems: (i) a high-temperature thermal insulation-covered cylindrical cell body made up of a reservoir containing about 700 g of silver and a 100 cm³ plasma reaction chamber; (ii) an inductively coupled heater to melt the silver which consists of 1/4" diameter copper tubing antenna that is tightly wrapped around the cell body to provide water cooling in addition to 30 kHz heating power; (iii) an electromagnetic pump to inject the molten silver upward between the tungsten electrodes, wherein oxide is added on-the-fly that is incorporated in the molten injection stream; and (iv) a super capacitor based ignition system to produce the low-voltage, high current flow across the pair of electrodes into which the molten metal and are injected in the presence of hydrogen to form the brilliant light-emitting plasma which characterizes the SunCell[®].

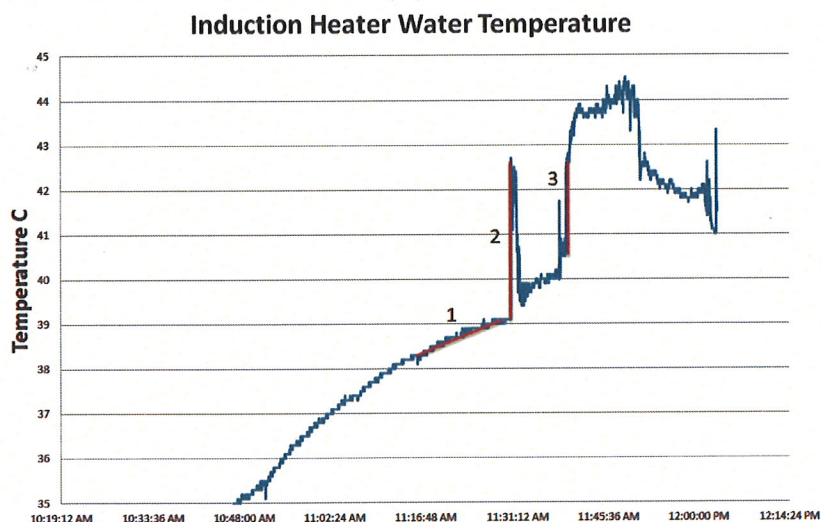
I was in the Brilliant Light Power lab when they ran three demonstrations of the SunCell[®]. The reaction occurs very abruptly, causing the cell to go from the nice red-orange color of the heating system of the silver to a very loud, explosive reaction that is green in color. At first, silver particles are seen to come off the open reaction cell. Then silver vapor is seen to come out at later times. In the first run the green explosive stage lasted for about 30 minutes – a long time! In the second run the green explosive stage lasted for about 10 minutes, then stopped abruptly. Pooling of liquid silver was seen at the bottom of the cell. This was a more intense run that created more heat and burned a hole through the reaction cell where the liquid silver ran out. When the liquid silver fuel left the reaction cell, there was no more fuel to sustain the reaction, and the reaction died out quickly. In the third run the green explosive stage only lasted for about 5-10 minutes until the reactor melted. The reaction quickly went away after that time. We were able to measure the power output of these reactions by monitoring the thermal coolant temperature response.

In the first run, 1 mole% H_2 was added to the molten silver (Test 052316PA1). The input power was 5.02 kW = 5,020 W, where 4.2 kW came from the inductively coupled heater and 0.820 kW came from the electromagnetic pump. When the SunCell[®] reaction begins, there's a change in slope. We compared the slope after the reaction starts to the slope before the reaction starts. This change in slope yields the power output of the SunCell[®]. The reaction of itself provides very little power and is negligible. The thermal burst power from this reaction was 3,200,000 W. This is 637.5 times more power generated than input! See Figure 5.

Figures 5A and 5B. 052316PA1 test of addition of 1 mole% to molten silver with 9 liter per min Ar/3% showing the temperature of the water in the antenna coil cooling loop of the inductively coupled heater as a function of time.



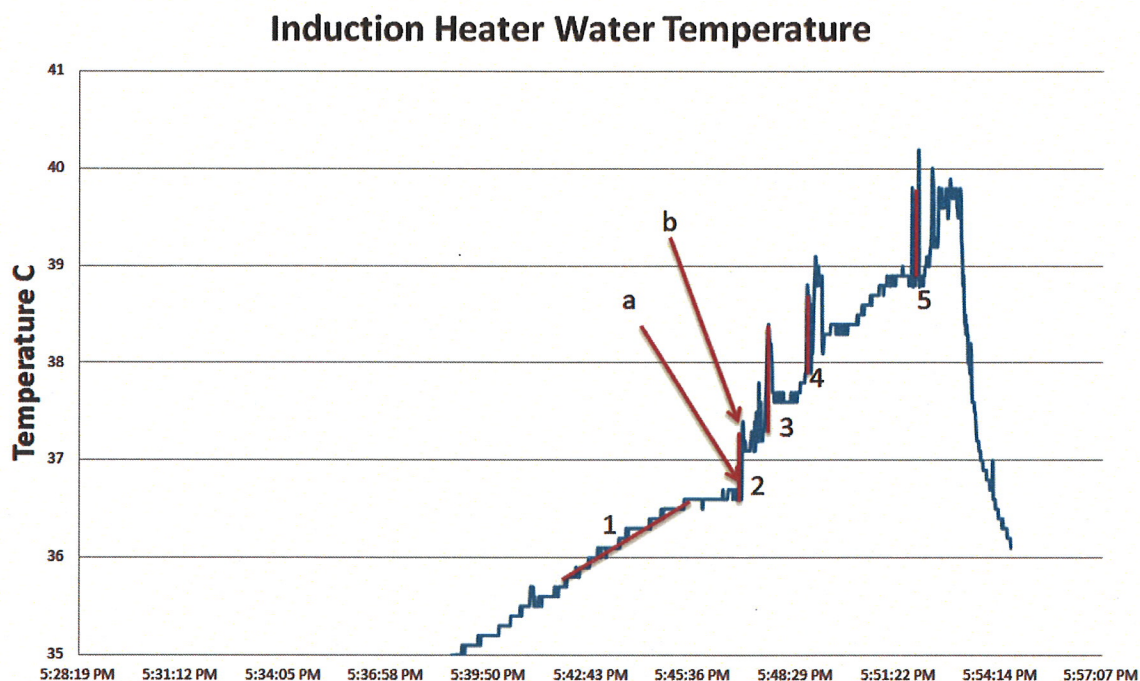
(A)



(B)

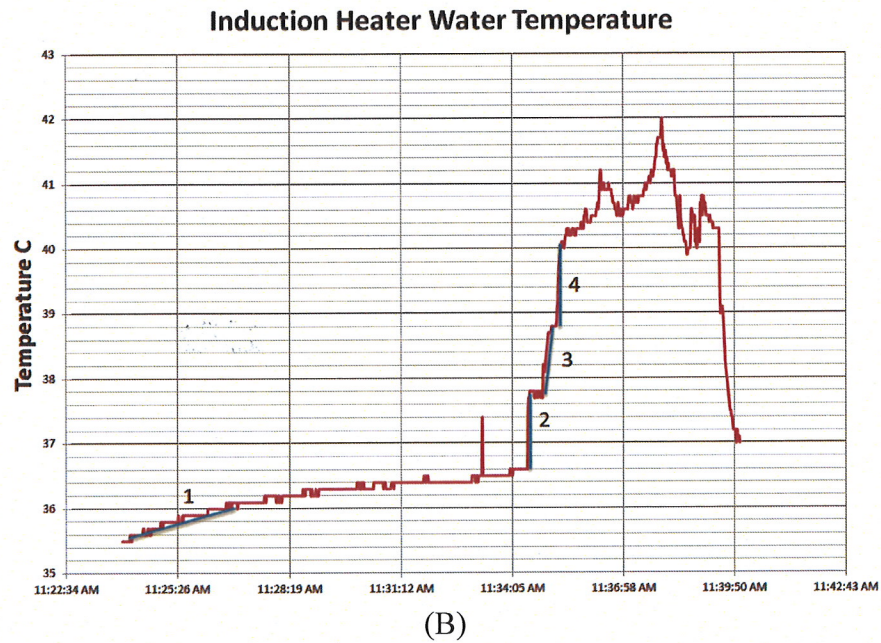
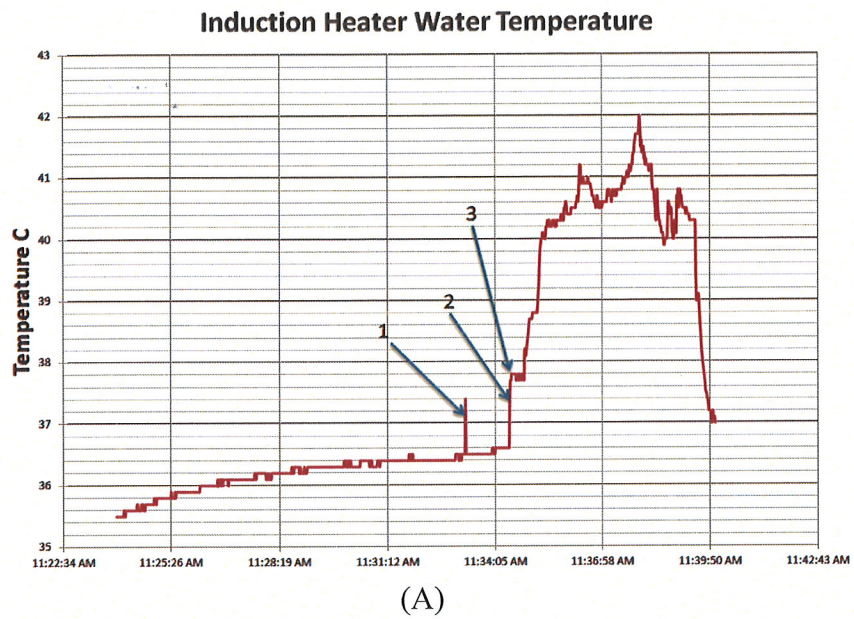
In the second run, 1mole% was added to the molten silver (Test 052316PA2). The input power was 9 kW, where 4.2 kW came from the inductively coupled heater, 4.0 kW average came from the electrodes, and 0.800 kW came from the electromagnetic pump. When the SunCell[®] reaction begins, there's a change in slope. We compared the slope after the reaction starts to the slope before the reaction starts. This change in slope yields the power output of the SunCell[®]. The thermal burst power from this reaction was 1,800,000 W. This is 200 times more power generated than input! See Figure 6.

Figure 6. 052316PA2 test of addition of 1 mole% LiVO_3 to molten silver with 9 liter per min Ar/3% showing the temperature of the water in the antenna coil cooling loop of the inductively coupled heater as a function of time. The coolant thermal responses as a function of time for the different experimental regimes were curve fit for thermal power determination: line 1 is the curve fit of the initial non-reaction period; line 2 is the curve fit of the reaction period following plasma initiation; lines 3, 4, and 5 are the curve fit of the power burst events during the reaction period post addition of



In the third run, 0.5 mole% LiVO_3 was added to the molten silver (Test 0524BDR). The input power was 8.79 kW, where 4.23 kW came from the inductively coupled heater, 3.76 kW average came from the electrodes, and 0.800 kW came from the electromagnetic pump. When the SunCell[®] reaction begins, again there's a change in slope. We compared the slope after the reaction starts to the slope before the reaction starts. This change in slope yields the power output of the SunCell[®]. The thermal burst power from this reaction was 230,000 W. This is 26 times more power generated than input! See Figure 7.

Figures 7A and 7B. 0524BDR test of addition of 0.5 mole% to molten silver with 9 liter per min Ar/3% showing the temperature of the water in the antenna coil cooling loop of the inductively coupled heater as a function of time.



Executive Summary

Brilliant Light Power has discovered a novel new heat and power source called the SunCell[®], which produces a tremendous excess of heat and power. These output power numbers listed above have been validated by me, and are correct. I have been given access to the data files for analysis. I am led to the conclusion that the generation of the net excess power and heat in the SunCell[®] experiment is real and reproducible.

APPENDIX A

Bomb Calorimetry on HOH-Based Hydrino Solid Fuels

Abstract: Using an oxide as a source of oxygen inside of a 2 mm diameter silver shot that served as a highly conductive matrix and an argon-hydrogen (95/5%) atmosphere as a source of atomic hydrogen, a hydrino HOH-based solid fuel formed when the shot was ignited by applying a current of about 20,000 A through the fuel. The fuel was held between two electrodes of a low-voltage, high current power source that applied the current inside the cell of a commercial bomb calorimeter. The energy released from a 10 microliter shot of about 80 mg by the nascent HOH catalyzed transition of H to hydrino state $H_2(1/4)$ was observed to be up to 171 J for a 1 ms ignition event corresponding to an average power of 171,000 W.

I. Introduction

A molecule that accepts $m \cdot 27.2 \text{ eV}$ from atomic H with a decrease in the magnitude of the potential energy of the molecule by the same energy may serve as a hydrino catalyst. The potential energy of H_2O is 81.6 eV [1]; so, the nascent H_2O molecule (not hydrogen bonded in solid, liquid, or gaseous state) may serve as a catalyst. Thermal energy was produced from the catalysis of H to $H(1/4)$ wherein nascent H_2O served as the catalyst, and a chemical reaction was the source of atomic hydrogen and catalyst. Solid fuels that form HOH catalyst and H showed multiple times the maximum theoretical energy [2]. Excess heats from solid fuels reactions were measured using water-flow calorimetry and these results have been independently confirmed by differential scanning calorimetry (DSC) runs at testing laboratories. The predicted molecular hydrino $H_2(1/4)$ was identified as a product of power producing cells, CIHT cells and thermal cells, by techniques such as MAS 1H NMR, electron-beam excitation emission spectroscopy, Raman spectroscopy, Raman spectroscopy with surface enhanced Raman scattering (SERS), time-of-flight secondary ion mass spectroscopy (ToF-SIMS), electrospray ionization time-of-

flight mass spectroscopy (ESI-ToFMS), Fourier transform infrared (FTIR) spectroscopy, X-ray photoelectron spectroscopy (XPS), and photoluminescence emission spectroscopy [2-5].

Based on the catalyst mechanism, high current facilitates a rapid transition rate (higher kinetics) by providing a sink for the inhibiting space charge build up from the ionization of the HOH catalyst. A solid fuel comprising a conductive matrix having, as a source of oxygen to react with H supplied by a argon-hydrogen atmosphere and further comprising some bound water was confined between two electrodes of a high current source (20,000 A) to form a low-voltage arc current to dissipate space charge from the hydrino reaction to support high kinetics. The energy balance and time of the event were separately determined by bomb calorimetry and by the mechanical disruption time of the voltage and current waveform by the blast event, respectively. From these parameters the power was determined.

II. Experimental

The energy balances were measured on the HOH-based solid fuel samples each comprising a silver shot of about 80 mg having 1 mol% on. The shots were formed by melting the silver and in a graphite crucible using an inductively coupled heater, rapidly quenching the molten mixture on an inert heat sink, and then punching the shot out of the solid slab. The shot comprised about 1 mole % water content determined by X-ray diffraction (XRD). Cylindrical copper caps of about 3.5g, 12 mm OD and 4 mm thickness served as the calibration control to determine the calorimeter heat capacity. Chromium metal flakes of about 2 mm thickness were used as a control that melted and produced an arc plasma. The cell gas for control cases was ultra-high purity Argon. The cell gas for non-control cases comprised argon-hydrogen (95/5%) at one atmosphere. Cell gas was introduced via positive pressure purging for 5 minutes at a flow rate of 4800 sccm.

The setup of the Parr 1341 calorimeter used for the energy balance determination (Figure 1) comprised an unmodified calorimeter jacket (21) and calorimeter cover (1) (combined Parr part number A1100DD) [3]. A thermistor with a temperature resolution of 0.001°C (2) (Parr part number 1168E2) passed through the calorimeter cover and was secured such that it read the water temperature in line with the bomb assembly at a distance of 2.54 cm from the bottom of the water bucket (19). The custom made, 0.051 cm thick stainless steel oval bucket weighed 417.8 g and had a small diameter of 12.7 cm inches, a large diameter of 18.4 cm, and a height of 10.2 cm. The water bucket held 1225±.01 g of deionized water along with the custom calorimeter bomb assembly. A stirring assembly (6) comprised a stirrer pulley (Parr part number 37C2), a stirrer bearing assembly (Parr part number A27A), and stirrer shaft with impeller (11) (Parr part number A30A3). It was mounted on the calorimeter cover and was connected to the motor assembly (Parr part number A50MEB) by a motor pulley (8) (Parr part number 36M4) by

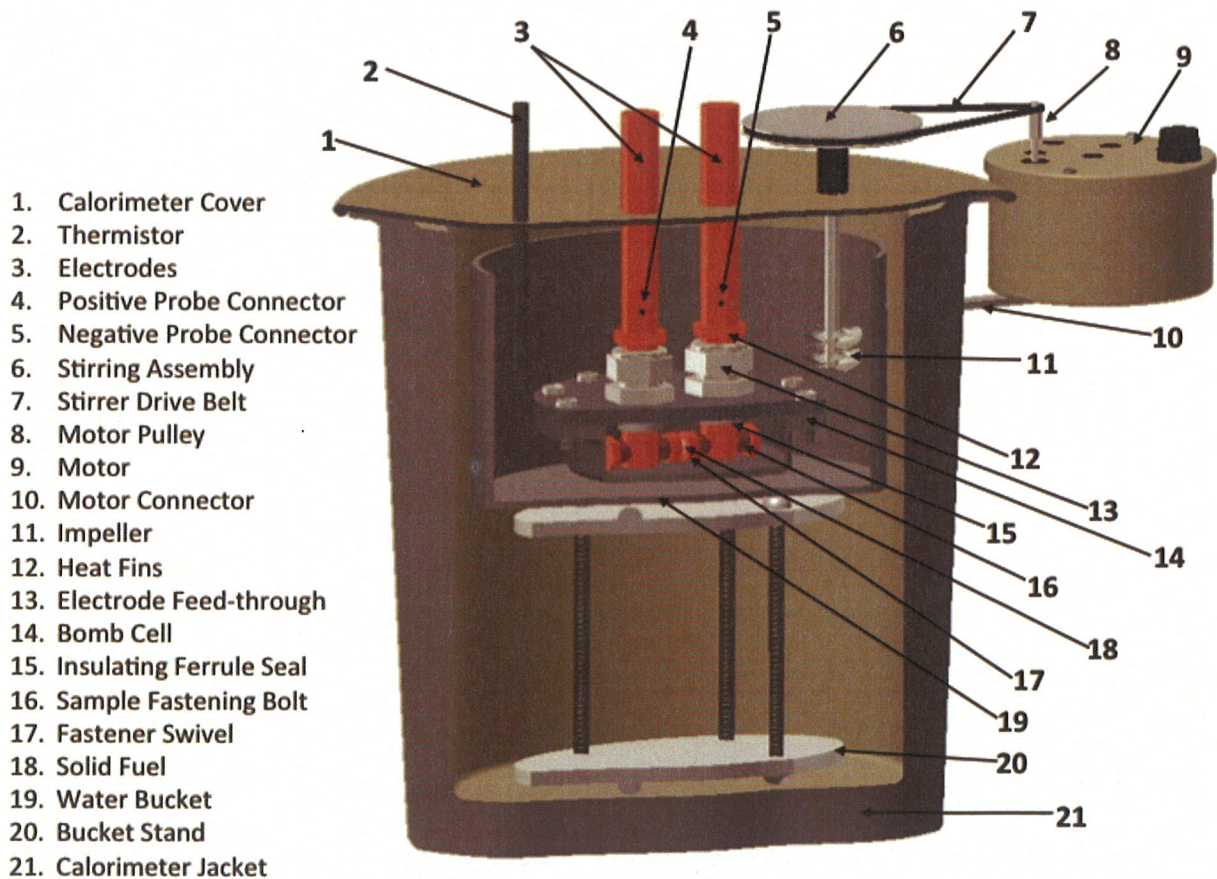
a stirrer drive belt (7) (Parr part number 37M2) driven by the motor (9). The motor assembly was attached to the calorimeter externally by an L-bracket motor connector (10) to prevent the heat output of the motor from affecting the calorimetric measurements. Two 1.6 cm OD silver-plated, hollow copper electrodes (3) passed through customized holes in the calorimeter cover and further passed through a Teflon position stabilizing block and then connected to the main conductors of an ACME 75 kVA resistance welder. The 0.32 cm thick stainless steel custom cylindrical bomb cell (14) had a 7.62 cm diameter and 2.54 cm height with a 12.4 cm flange that was 0.64 cm thick. The electrodes penetrated the flange lid through electrode feed-throughs (13) with Teflon insulating ferrule seals (15) that provided electrical isolation and a hermetic seal. Power was transmitted to the solid fuel (18) with or without the 1.3 cm diameter 0.48 cm thick copper fastener swivel (17) by the 3.0 cm long, 0.95 cm diameter copper sample-fastening bolts (16) which were threaded through the base of the electrodes. The solid fuel was contained between the fastener swivels by tightening the sample fastening bolts to a torque of approximately 1.81 Nm as measured by a high accuracy flat beam torque wrench resulting in approximately 1112 N force to the sample as measured by a piezoresistive force sensor (Measurement Specialties, FC2311-0000-0250-L). Efficient heat transfer was enabled by heat fins (12) installed on the electrodes immediately above the electrode feed-throughs that ensured minimal heat loss through the electrodes and out of the closed system. The bucket stand (20) elevated the bomb cell to the top of the calorimeter to minimize the dimensions and quantities of materials necessary to operate the Parr 1341 calorimeter and improve the accuracy of the measurements.

Each sample was ignited with an applied peak 60 Hz voltage of less than 10 V and a peak current of about 20,000 A. The input power was recorded through a custom interface receiving input from the positive probe connector (4) and negative probe connector (5). The input energy of the calibration and ignition of the solid fuel was given as the product of the voltage and current integrated over the time of the input. The voltage was measured by a data acquisition system (DAS) comprising a PC with a National Instruments USB-6210 data acquisition module and Labview VI. The current was also measured by the same DAS using a Rogowski coil (Model LFR15/150/700) that was accurate to $\pm 0.3\%$ as the signal source. V and I input data were obtained at 83 KS/s and a voltage attenuator was used to bring analog input voltage to within the ± 10 V range of the USB-6210.

The input power data was processed to calculate the input energy during the rapid power decay following ignition to an open circuit. Taking the product of the measured voltage waveform obtained from the voltage taps immediately above the water level on the 5/8" OD Cu rods and the measured current waveform given by the Rogowski coil yielded the power waveform. The time integrated power waveform yielded the cumulative energy provided to the

system to the time point that the ignition or detonation event occurred. The secondary circuit of the spot welder transformer was temporarily broken as the electrode tips were pushed apart by the force of the blast. On a time scale of about $10\ \mu\text{s}$, the circuit quickly transitioned to high resistance, effectively becoming an open circuit with the development of a reactive voltage transient as a result of the fast collapsing magnetic flux in the transformer. The current fell to zero as the voltage transient produced a corresponding reflected wave reactive power component in the power waveform that typically rapidly decayed on the order of about $500\ \mu\text{s}$ to $1\ \text{ms}$. To eliminate this reactive power component over the time of the current decay, the power waveform was smoothed over the immediate post-blast period until current reached zero by fitting the voltage and current components during this time to their typical amplitudes and phases during pre-blast conditions. The accuracy of this method was confirmed by the achievement of energy balance with control samples.

Figure 1. The setup of the Parr 1341 calorimeter used for the energy balance determination.



III. Results and Discussion

Using the Cu metal caps in Table 1, the heat capacity of the calorimeter and electrode apparatus used to measure the energy balance of solid fuel samples was determined to be 6400 J/°C. The calorimetry method used to determine the thermal output from the temperature versus time response following equilibration and ignition was the analytical method described in the operating manual of the Parr 1341 bomb calorimeter [6]. The net energy is the difference between the thermal output and energy input.

As shown in Table 1, near zero net energy balance was measured on the control Cr foil flakes. In contrast, significant energy and power was observed for the HOH-based solid fuel wherein HOH served as catalyst. Up to 171 J was recorded for a 1 ms ignition event corresponding to an average power of 171,000 W. The power from other methodologies such as absolute spectroscopy on the ignition of hydrated silver shot and the coolant thermal response with the addition of an oxide to an injected molten silver stream exposed to argon-H₂ (95-5%) flow was higher due to the larger reaction volumes compared to the limited-volume calorimetric cell. Moreover, the net energy could be higher than reported considering that a significant portion of the input energy was dissipated in the two joints and the bus bars of the calorimeter fuel ignition circuit with only about 50% of the input energy actually delivered to the fuel sample to cause it to ignite. For no theoretical energy exits since the no exothermic reaction was possible between argon, hydrogen, and silver.

References

1. R. Mills, *The Grand Unified Theory of Classical Physics*; 2014 Edition, posted at <http://www.blacklightpower.com/theory-2/book/book-download/>.
2. R. Mills, J. Lotoski, W. Good, J. He, "Solid Fuels that Form HOH Catalyst," *Int'l J. Hydrogen Energy*, 39 (2014), pp. 11930–11944 DOI: 10.1016/j.ijhydene.2014.05.170.
3. R. Mills J. Lotoski, "H₂O-based solid fuel power source based on the catalysis of H by HOH catalyst", *Int'l J. Hydrogen Energy*, Vol. 40, (2015), 25-37.
4. R. Mills, X Yu, Y. Lu, G Chu, J. He, J. Lotoski, "Catalyst induced hydrino transition (CIHT) electrochemical cell," (2012), *Int. J. Energy Res.*, (2013), DOI: 10.1002/er.3142.
5. R. Mills, J. Lotoski, J. Kong, G. Chu, J. He, J. Trevey, "High-Power-Density Catalyst Induced Hydrino Transition (CIHT) Electrochemical Cell." *Int. J. Hydrogen Energy*, 39 (2014), pp. 14512–14530 DOI: 10.1016/j.ijhydene.2014.06.153.
6. <http://www.parrinst.com/products/oxygen-bomb-calorimeters/1341-plain-jacket-bomb-calorimeter/>.

Table 1. Determination of the energy balance of the hydrino solid fuel by bomb calorimetry.

Experiment and Description	Purpose	Purge	VI Energy Input (J)	VI Power Fitted Energy Input (J)	Room Temp @ Fire Time (°C)	Event Duration (End-Fire time) (min)	Total dT (°C)	Parr Calc'd dT (°C)	Pre Slope (°C/min)	Post Slope (°C/min)	Thermal Energy Out (J)	VI Power Fitted Energy Input (J)	VI Power Fitted Energy Gain (X)	VI Power Fitted Energy Net (J)	VI Energy Input (J)	VI Energy Gain (X)	VI Energy Net (J)
2016-05-24-MY4 Cr flake control 77.9 mg ("2.8 x 3.0 x 2.3 mm), 55 lbs.	Testing disruptive control	5min UHP Ar	284.0	256.6	23.84	4.22	0.0340	0.0405	-0.002293	-0.001454	259.3	256.6	1.01	2.6	284.0	0.91	-24.7
2016-05-24-MY3 Ag (1 mol%) pellet, 76.4 mg, 175 lbs.	Testing batch 051716RF2 Ag (1 mol%) pellet	5min 5% H2:Ar	377.7	230.6	23.59	5.98	0.0530	0.0606	-0.001821	-0.001095	387.9	230.6	1.68	157.3	377.7	1.03	10.2
2016-05-24-MY1 Ag (1 mol%) pellet, 75.0 mg, 175 lbs.	Testing batch 040816CC1 Ag (1 mol%) pellet	5min 5% H2:Ar	368.5	196.6	23.05	5.60	0.0520	0.0574	-0.001633	-0.000821	367.6	196.6	1.87	171.0	368.5	1.00	-0.9
2016-05-23-MY3 Cr flake control 81.0 mg ("2.9x2.6 x 2.1 mm), 55 lbs.	Testing disruptive control	5min UHP Ar	270.0	234.5	23.54	7.10	0.0300	0.0374	-0.001589	-0.000833	239.1	234.5	1.02	4.5	270.0	0.89	-30.9
2016-05-24-MY2 Ag (1 mol%) pellet, 75.0 mg, 175 lbs.	Testing batch 040816CC1 Ag (1 mol%) pellet	5min 5% H2:Ar	376.5	208.1	23.35	6.88	0.0520	0.0587	-0.001893	-0.000748	375.5	208.1	1.80	167.4	376.5	1.00	-1.0
2016-05-23-MY1 Cu Caps control, 175 lbs.	Testing resistive control	5min UHP Ar	248.4	248.4	23.03	5.85	0.0360	0.0412	-0.001556	-0.000654	263.6	248.4	1.06	15.2	248.4	1.06	15.2

APPENDIX B

Power Determination of the Light Released from Ultra-low Field Ignition of Hydrated Silver Shots Using Absolute Spectroscopy over the 22.8-647 nm Wavelength Range

Abstract: Extreme ultraviolet (EUV) continuum radiation (10-30 nm) arising only from very low energy pulsed pinch gas discharges comprising some hydrogen was first observed at Brilliant Light Power, Inc. and reproduced at the Harvard Center for Astrophysics (CfA). The source was determined to be due to the HOH catalyzed transition of H to the lower-energy hydrogen or hydrino state H(1/4). The HOH catalyst was further shown to give EUV radiation of the same nature by igniting hydrated silver shots comprising a source of H and HOH catalyst by passing a low voltage, high current through the shot to produce explosive plasma that emitted brilliant light predominantly in the short-wavelength 10 to 300 nm region. The power and energy of the light released from the shot ignition event were determined using absolute spectroscopy over the 22.8-647 nm region. The peak and average powers of the light released from the shot ignition event determined using absolute spectroscopy over the 22.8-647 nm region were 2.1 MW and 514,700 W corresponding to 83.6 J in 40 us and 350 J in a 0.68 ms blast event, respectively. It was remarkable that the radiation was essentially all short wavelength in the EUV and UV range with essentially no visible or near infrared light. The power density was high considering the source of the more than 514,700 W was a shot of less

than 10 microliter volume. This result is even more extraordinary considering the peak power was 1.3 MW. Using the Mightex UV-Vis spectrometer, absolute spectroscopy was also recorded over the wavelength range of 200-816 nm on ignited partially hydrated 80-90 mg silver (3 mole %) and silver- (1-3 mole %) shots. The peak optical power in the UV-visible of about 689,000 W exceeded the ignition input power of 25 kW even considering that the UV-visible light power represents only about 25% of the total optical power extending to 10 nm. Suppressing hydrino reactant atomic hydrogen essentially eliminated the optical power.

I. Introduction

Atomic hydrogen is predicted to form fractional Rydberg energy states $H(1/p)$ called "hydrino atoms" wherein $n = \frac{1}{2}, \frac{1}{3}, \frac{1}{4}, \dots, \frac{1}{p}$ ($p \leq 137$ is an integer) replaces the well-known parameter $n = \text{integer}$ in the Rydberg equation for hydrogen excited states. The transition of H to a stable hydrino state $H\left[\frac{a_H}{p = m+1}\right]$ having a binding energy of $p^2 \cdot 13.6 \text{ eV}$ occurs by a nonradiative resonance energy transfer of $m \cdot 27.2 \text{ eV}$ (m is an integer) to a matched energy acceptor. The nascent H_2O molecule (not hydrogen bonded in solid, liquid, or gaseous state) may serve as a catalyst by accepting 81.6 eV ($m = 3$) to form an intermediate that decays with the emission of a continuum band with a short wavelength cutoff of 10.1 nm and energy of 122.4 eV [1-6]. The continuum radiation band at 10.1 nm and going to longer wavelengths for theoretically predicted transitions of H to lower-energy, so called "hydrino" state $H(1/4)$, was observed only arising from pulsed pinch gas discharges comprising some hydrogen first at BlackLight Power, Inc. (BLP) and reproduced at the Harvard Center for Astrophysics (CfA) by P. Cheimets and P. Daigneau [5]. The source was determined to be due to the HOH catalyzed transition of H to the lower-energy hydrogen or hydrino state $H(1/4)$. The HOH catalyst was further shown to give EUV radiation of the same nature by igniting hydrated silver shots comprising a source of H and HOH catalyst by passing a low voltage, high current through the shot to produce explosive plasma that emitted brilliant light predominantly in the short-wavelength 10 to 300 nm region. The power and energy of the light released from the shot ignition event were determined using absolute spectroscopy over the 10-816 nm region using a grazing incidence EUV spectrometer (GIS), normal incidence EUV spectrometer (NIS), and a ultraviolet-visible (UV-Vis) spectrometer wherein the UV-Vis spectrometer was absolutely calibrated using a NIST traceable tungsten lamp and

a deuterium lamp. The intensity calibration was extended to the EUV wavelengths by spectral overlap with calibrated regions and the spectral responses of the spectrometers.

The optical power was further recorded in the ultraviolet region with partially hydrated 80-90 silver (3 mole %) and silver (1-3 mole %) shots that provided the hydrino reactants of H and HOH, and the UV power was compared to the ignition power as different atmospheres were tested that would alter hydrino reaction kinetics. The results of vacuum was used to provide predominantly atomic hydrogen for water of hydration to enhance the kinetics was compared to the results with 100% H₂ comprising essentially all molecular hydrogen with suppression of atomic hydrogen.

II Experimental Method: Absolute Power Spectrum of Ignited Hydrated Silver Shots

Schematics of the light source comprising hydrated silver shot ignited with a spot welder, the intensity reducing, evacuated light conduit, and each of the spectrometers, ultraviolet-visible, normal incidence, and grazing incidence to cover the wavelength range 10-816 nm are shown in Figures 1A, 1B, and 1C, respectively. Silver shots of about 1.24 mm radius, weighing about 80-90 mg were formed by dripping molten silver through a 0.1 mm diameter dripper into distilled water maintained at room temperature. The shots were retrieved and agitated to remove excess water, but were not dried. The shot water content was determined to be about 1 mole% by weighing about 10 g of shots before and after melting them in the glove box wherein the weight loss was attributed to the removed the water. The shots were singly fired in a vacuum chamber (14.6 cm diameter X 28 cm length) with a windowless connection to the vacuum tube (3.5 cm ID) that was either connected to the GIS, the NIS (EUV wavelengths), or a MgF₂ window (7 mm diameter, 2 mm thickness) that was incident to the entrance optics of the NIS (UV-Vis wavelengths) or the Mightex spectrometer. The chamber and tube were evacuated to 1×10^{-3} Torr (NIS and UV-Vis) or 5×10^{-4} Torr (GIS) as different spectral regions were acquired. The EUV spectrometers were differential pumped to 1×10^{-6} Torr in order to record the EUV wavelengths. Each shot was confined between the two copper electrodes of a spot welder (Taylor-Winfield model ND-24-75 spot welder, 75 KVA, 15 PSI applied electrode pressure) wherein the electrodes penetrated the vacuum chamber at vacuum-sealed, electrically insulating penetrations. The horizontal plane of the sample was aligned with the optics of each spectrometer as confirmed by an alignment laser. Each sample was subjected to a short burst of low voltage, high current electrical energy. The applied 60 Hz AC voltage was less than 1 V across the shot, and the peak current was about 23,000-25,000 A at an applied total voltage of about 6 V. The high current caused the sample to ignite as brilliant light-emitting expanding dense plasma. To cause the plasma to become optically thin such that EUV light could emerge, the ignition occurred in the 4.7 liter vacuum chamber that housed the ignited sample. The plasma density decreased with rapid expansion to become transparent.

The EUV spectrum (5-65 nm) was recorded using a McPherson grazing incidence EUV spectrometer (Model 248/310G) equipped with a 600 g/mm gold coated grating. The angle of incidence was 87°. The wavelength resolution with an entrance slit width of 200 μm was about 0.3 nm at the CCD center and 0.7 nm at the limits of the CCD wavelength range window of 50 nm. A 150 nm thick aluminum filter (Luxel Corporation) was placed between the grating and CCD detector to block the visible light and to prevent damage to the spectrometer from the blast debris. The transmittance of the Al filter has a transmission window between 17 nm to 80 nm as shown in Figure 2A. To measure to the 10.1 nm short wavelength cutoff of the H(1/4) transition continuum radiation while selectively blocking visible light, a 150 nm thick Zr filter (Luxel Corporation) was placed in the light path between the grating and CCD detector. The transmittance of the Zr filter has a transmission window in the region of 10 nm as shown in Figure 2B. The evacuated distance from the shot to the slits was 1.48 m. The EUV light was detected by a CCD detector (Andor iDus) cooled to -60 °C. The CCD detector was centered at 25 nm and 55 nm to cover the wavelength region of 0-65 nm. Known oxygen and nitrogen ion lines observed in a high voltage pulse discharge spectrum were used to calibrate the wavelengths of the 0 to 65 nm region prior to recording the shot blast spectrum.

The shot light emission was introduced to a normal incident EUV spectrometer for spectral measurement of the wavelength region covered by the monochromator of 30-650 nm. The spectrometer was a McPherson 0.2 meter monochromator (Model 302, Seya-Namioka type) equipped with a 300 g/mm Al-MgF₂ coated grating. The EUV light was detected by the Andor iDus CCD camera. The slits were set at $\sim 10 \mu\text{m}$. The vacuum inside the monochromator was maintained below 1×10^{-6} Torr by a turbo pump. The evacuated distance from the shot to the slits was 1.20 m. The calibration of the spectral intensity was obtained by matching the intensity in regions of wavelength overlap (210.8 to 647 nm) with the spectrum of a UV-Vis spectrometer that was calibrated with a NIST traceable quartz tungsten halogen lamp and a deuterium/W lamp.

The shot light emission was introduced to a UV-Vis Mightex system spectrometer for spectral measurement of the wavelength region 200-816 nm that was calibrated with NIST traceable W and deuterium/W lamp lamps. The Mightex system is comprised (i) a Horiba MicroHR f/3.9 imaging spectrometer (Model: MHR-MS) with variable entrance slit from 10 μm to 2 mm width by 1 mm or 3 mm high and a 150 g/mm ruled grating blazed at 500 nm, (ii) a Mightex buffered and triggerable USB 2.0 CCD linescan camera (Model: TCE-1024-UF) with 1024 pixels of 14 x 14 μm size per pixel, spectral range from 200 to 1000 nm, 8 bit ADC at 25 kFPS, and 40 μs minimum exposure time, and (iii) a MgF₂ window (7 mm diameter, 2 mm thickness) on the entrance to the spectrometer and a fused silica window on the entrance of the camera. The Mightex was triggered by a 30 μs duration 5V signal generated by an Agilent 33220A 20 MHz Arbitrary Waveform

Generator when a gating signal generated by a Picoscope 5442B digital oscilloscope was issued when current began to flow above a threshold in the welder as measured by a Rogowski current probe (Model: PEM LFR15/150/700).

The parameters during acquisition and data processing of the GIS-NIS-Mightex acquisition sequence as used by the Mightex were: the Horiba spectrometer center was 500 nm, the slit width was 30 μm , the slit height was 1 mm, the exposure time was 40 μs , the frame rate was 25,000 frames/s (FPS) wherein 2000 frames were acquired over an 80 ms acquisition time, the evacuated path distance from the silver shot to the MgF_2 window was 1.15 m, the light exited the window to travel 0.05 m in air to the Mightex slits such that the total distance from the shot to the slits was 1.20 m, and the absolute irradiance integration range was 200-816 nm. The spectra were wavelength calibrated using emission lines generated by a mercury argon wavelength calibration source (Model: Ocean Optics HG-1). A 3rd order polynomial was used to generate the pixel to wavelength mapping. The absolute intensity calibration was performed using a Newport Calibrated Source Lamp, Quartz Tungsten Halogen (QTH), 1000 W, confirmed calibration to NIST traceable standards over 250-2400 nm, (Model: 63350). The QTH calibration lamp setup was described previously [7]. The instrument response function of the Mightex absolute irradiance calibration using the QTH lamp was extended to 200 nm using a Hamamatsu L10290 D2/W combo source with known relative irradiance by direct coupling to the Mightex. The relative irradiance of the Hamamatsu source was matched to the absolute irradiance in the region of 350 nm as calibrated by the QTH lamp to determine the UV region instrument response function.

The 5 nm to 65 nm region was recorded with the GIS. The CCD dark counts were subtracted from all spectra. The spectrum recorded with the CCD centered at 25 nm using the Zr filter (Figure 2B) was corrected by dividing the data by the wavelength-matched Zr filter curve. The spectrum recorded with the CCD centered at 55 nm using the Al filter was corrected by dividing the data by the Al filter curve (Figure 2A). Matching the intensities at overlapping spectral wavelengths was used to join the 25 nm and 55 nm curves. The joined spectrum was corrected for the efficiency of the Au coated 600 g/mm grating by dividing the data by the grating efficiency curve (Figure 3). The wavelength calibration was achieved using the spectrum from a high voltage discharge in air (Figure 4).

The 25 nm to 650 nm region was recorded with the NIS. The CCD dark counts were subtracted from all spectra. Spectra were recorded with the CCD centered at 100, 200, 300, 400, and 500 nm using the MgF_2 window except in the case of the 100 nm and 200 nm spectra since those wavelengths were cutoff by the window (Figure 5). Matching

the intensities at overlapping spectral wavelengths was used to join the spectrum acquired at CCD center positions. The joined spectrum was corrected for the reflectance but not the efficiency of the NIS 300G Al-MgF₂ coated grating by dividing the data by the grating reflectance curve (Figure 6) only. The spectrum was not corrected for the grating efficiency curve shown in Figure 6 since it was a theoretical curve provided by the vendor McPherson and was not well known to short wavelengths (<200 nm) where the most significant correction exists. Work is in progress to use the SunCell[®] blackbody curve in the deep UV to calibrate the grating efficiency.

Matching the intensities at overlapping spectral wavelengths was used to join the corrected curves of the GIS and the NIS. The joined spectrum was corrected for the efficiency of the CCD by dividing the data by the wavelength-matched CCD quantum efficiency curve (Figure 7). The spectral count intensity was converted to energy density by multiplying the counts as a function of wavelength by the conversion factor $\frac{hc}{\lambda}$.

The 200 nm to 816 nm region was recorded with the Mightex UV-Vis spectrometer using the MgF₂ window. The spectrum was corrected by dividing the data by the transmission efficiency of the window (Figure 5). The UV-Vis spectral results were used to scale the GIS-NIS combined spectrum to achieve a match in the spectral overlap region. The integrated power of the Mightex spectrum was determined over the wavelength region 210.8-647 nm. The GIS-NIS spectrum was scaled such that the integrate power in the 210.8-647 nm region matched that of the Mightex spectrum. The total power over the full wavelength range of 22.8-647 nm was integrated on the combined spectrum.

Using the Mightex UV-Vis spectrometer, absolute spectroscopy was also recorded over the wavelength range of 200-816 nm on ignited partially hydrated 80-90 mg silver- AgNO_3 (3 mole %) and silver- AgNO_3 (1-3 mole %) shots. The salt-containing shots were formed by mixing the salt into molten silver in a graphite crucible maintained at 1100 °C in the glove box by an inductively coupled heater. The melt was rapidly quenched on a stainless steel metal block, and shots were produced with a metal punch. The shot comprised about 1 mole % water content determined by X-ray diffraction (XRD). Using the spot welder, the shots were ignited in the chamber having the windowless connected vacuum-capable tube with the MgF₂ window at the far end from which light entered the Mightex spectrometer. The shots were run under vacuum and 1 atm pure H₂. The power of the spot welder was recorded as a function of time at a time resolution of 56 or 104 ns via 60 MHz digital oscilloscope (Picotech, Picoscope 5442B) using a voltage and current probe. The voltage was measured by a 25 MHz 70V 10:1

differential voltage probe (Picotech, model TA041) accurate to $\pm 2\%$ and the current was measured with a Rogowski coil (PEM, LFR 15/150/700) that was accurate to $\pm 0.3\%$. The light power was recorded as a function of time with the Mightex on a $40\ \mu\text{s}$ time scale and compared to the ignition power at the same time point of maximum power emission.

III. Results and Discussion

The hydrated silver shots comprising a source of H and HOH hydrino catalyst were ignited by passing a low voltage, high current through the shot to produce explosive plasma that emitted brilliant light predominantly in the short-wavelength (10 to 300 nm) region. The GIS was corrected for the Al and Zr filter curves shown in Figure 2A-B as well as for the grating efficiency (Figure 3). The NIS data was corrected by the MgF_2 window attenuation using data with and without the window. The NIS spectrum was further corrected by the reflectance curve but not the efficiency curve of the Al- MgF_2 coated 300 g/mm grating shown in Figure 6. The UV-Vis spectrum was corrected for the MgF_2 window transmission curve shown in Figure 5 and was absolutely calibrated. The raw spectra obtained using the GIS and NIS is shown in Figure 8. The combined GIS and NIS spectra following filter, grating, and CCD quantum efficiency corrections is shown in Figure 9. Figure 10 shows the combined GIS and NIS spectra before power calibration against the absolutely calibrated UV-Vis spectrum wherein the spectral count intensity of Figure 9 was converted to energy density by multiplying the counts as a function of wavelength by the conversion factor $\frac{hc}{\lambda}$.

The Mightex UV-Vis (200-816 nm) spectrum was corrected by dividing the data by the transmission efficiency of the window (Figure 5). The UV-Vis spectral results used to scale the GIS-NIS combined spectrum to achieve a match in the spectral overlap region were a peak emission power (40 μs resolution) of 319.5 kW, a total emission energy of 86.2 J, a total emission time of 0.68 ms, and a time averaged emission power of 126.7 kW. The integrated power of the Mightex spectrum was determined over the wavelength region 210.8-647 nm. The GIS-NIS spectrum was scaled such that the integrated power in the 210.8-647 nm region matched that of the Mightex spectrum. The total power over the full wavelength range of 22.8-647 nm was integrated on the combined spectrum. The full wavelength calibrated and absolute intensity calibrated emission spectrum (22.8-647 nm) is shown in Figure 11. The peak and average powers of the light released from the shot ignition event determined using absolute spectroscopy

over the 22.8-647 nm region were 2.1 MW and 514,700 W corresponding to 83.6 J in 40 us and 350 J in a 0.68 ms blast event, respectively.

In addition to the transmission and efficiency of the optical collection and recording components of the spectroscopy systems, a number of other factors should be considered in the power determination. The power from arc plasma driven by an axial electric field can be emitted in a dipole distribution that results in a $\cos^2\theta$ power distribution and a 1/4 total power correction from that measured at the peak intensity. However, as evidenced by high speed photography, the nature of the emission in the case of the shot ignition is an explosion with a spherical wave that propagates out in all directions uniformly except where it is blocked by a physical object such as the electrodes where the power is absorbed to result in recoil of the welder arms and electrodes and molten silver coating, evulsion, and melting of the copper electrodes. The optical power determination was under determined by a plurality of mechanisms. The NIS spectrum was only corrected for the 300G Al-MgF₂ coated grating reflectance (Figure 6, upper trace) and not the efficiency as well (Figure 6, lower trace). The efficiency was only known theoretically as provided by McPherson and was not well known especially at short wavelengths wherein significant corrections and resulting increases in intensity are expected. Further reducing the spectral intensity, the grating had lost some efficiency in the short wavelength region due to Ag coating it. This can be appreciated by comparing the short wavelength region spectrum shown in Figure 11 with a spectrum taken at an earlier time when the grating had less exposure to Ag blast debris (Figure 12). There are three additional factors that were not quantified that diminish the reported power below that actually emitted by the shot blast event: (i) The solid angle for light collection by the spectrometers is greatly reduced by electrode shadowing. It was found that if the electrodes were not beveled, essentially no light gets out. (ii) A related issue with the use of the 1.6 cm diameter electrodes, the great separation distance, and very narrow slits is that the electrodes block the light by reducing the solid angle such that sample-spectrometer alignment is critical. It was very likely that the light was recorded off angle from the sample plane at a diminished light intensity due to electrode shadowing since it is very difficult to perfectly align on axis especially given the movement with the blast event. (iii) The blast vapor and debris are optically thick until the plasma expands to become thinner. In fact, no EUV light was initially observed until a vacuum chamber was used to allow the plasma to expand to become thin enough for the EUV transparency. A substantial amount of the EUV light is absorbed when the power is the greatest in the first time increment following the blast and before transparency is achieved.

It was remarkable that the radiation was essentially all short wavelength in the EUV and UV range with essentially no visible or near infrared light (Figure 11). The power density was high considering the source of the more than 514,700 W was produced by a shot of less than 10 microliter volume. This result is even more extraordinary considering the peak power was 1.3 MW.



To search for the 10.1 nm short wavelength cutoff of the H(1/4) transition continuum radiation while selectively blocking visible light, a 150 nm thick Zr filter (Luxel Corporation) that has a transmission window in the region of 10 nm (Figure 2B) was placed in the light path between the grating and CCD detector. The emission spectrum of the hydrated Ag shot plasma emission using a grating that was not degraded in the short wavelengths showed strong EUV continuum having a 10.1 nm cutoff as predicted [1-4] as shown in Figure 12.



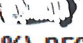

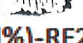

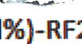
The results of the absolute spectroscopy (200-816 nm) recorded on ignited partially hydrated 80-90 mg silver-3 mole % and silver-1-3 mole % shots are given in Table 1. The peak power of the shots of about 689,000 W (40 us time resolution) was higher than the non-reactive ignition power of 25,000 W (104 us time resolution). The total optical power of the 22.8-647 nm region was shown to be about 4.1 times the optical power in the UV (>200 nm) range; so the total peak optical power is much higher, greater than 2.8 MW. It was found that a pure H₂ atmosphere that favored molecular hydrogen and suppressed the atomic H hydrino reactant essentially eliminated the optical power.

References

1. R. L. Mills, Y. Lu, "Hydrino continuum transitions with cutoffs at 22.8 nm and 10.1 nm," *Int. J. Hydrogen Energy*, 35 (2010), pp. 8446-8456, doi: 10.1016/j.ijhydene.2010.05.098.
2. R. L. Mills, Y. Lu, K. Akhtar, "Spectroscopic observation of helium-ion- and hydrogen-catalyzed hydrino transitions," *Cent. Eur. J. Phys.*, 8 (2010), pp. 318-339, doi: 10.2478/s11534-009-0106-9.
3. R. L. Mills, Y. Lu, "Time-resolved hydrino continuum transitions with cutoffs at 22.8 nm and 10.1 nm," *Eur. Phys. J. D*, Vol. 64, (2011), pp. 65, DOI: 10.1140/epjd/e2011-20246-5.
4. R. L. Mills, R. Booker, Y. Lu, "Soft X-ray Continuum Radiation from Low-Energy Pinch Discharges of Hydrogen," *J. Plasma Physics*, Vol. 79, (2013), pp 489-507; doi: 10.1017/S0022377812001109.

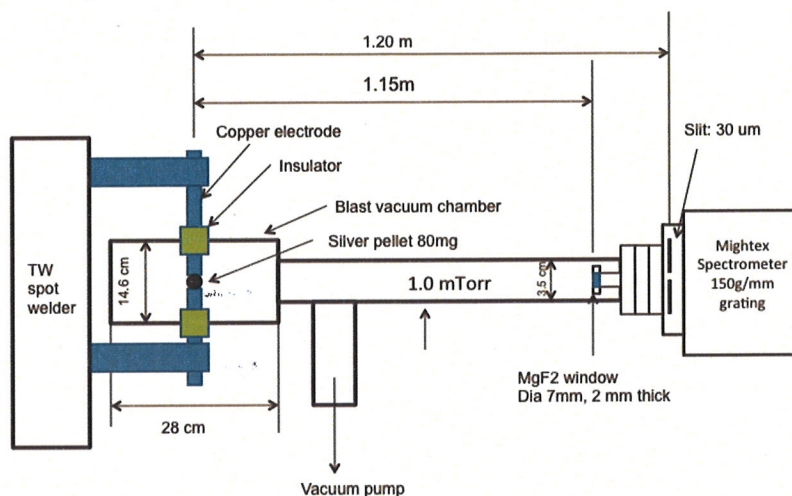
5. A. Bykanov, "Validation of the observation of soft X-ray continuum radiation from low energy pinch discharges in the presence of molecular hydrogen," http://www.blacklightpower.com/wp-content/uploads/pdf/GEN3_Harvard.pdf.
6. R. Mills, J. Lotoski, Y. Lu, "Mechanism of soft X-ray continuum radiation from low-energy pinch discharges of hydrogen and ultra-low field ignition of solid fuels", (2016), submitted, http://brilliantlightpower.com/wp-content/uploads/papers/Cont_EUV_HOH-031215.pdf.
7. Newport Light Sources document, Figure 2 (page 16: http://assets.newport.com/webdocuments-en/images/light_sources.pdf).

Table 1. The results of the absolute spectroscopy recorded on ignited hydrated silver shots, at least partially dehydrated silver shots, and partially hydrated 80-90 mg silver- (3 mole %) and silver- (1-3 mole %) shots over the wavelength range of

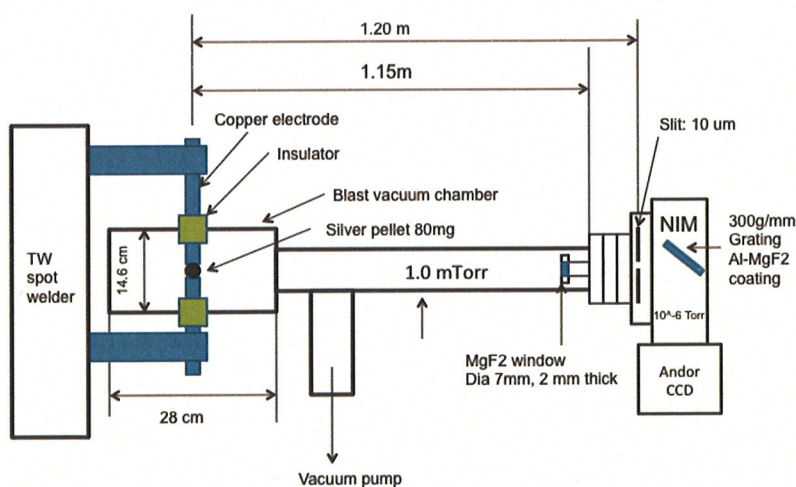
Setup Atm	Sample Type	Sample Mass (mg)	Peak Waveform Current (kA)	Mightex Energy (J)	Mightex Max Power (kW)
H2	Ag+  (3mol%)-RF1	85.0	22.9	28.4	176.0
H2	Ag+  (3mol%)-RF2	82.0	22.1	16.8	94.8
Vacuum	Ag+  (3mol%)-RF0	87.0	22.2	92.0	382.0
Vacuum	Ag+  (3mol%)-RF2	88.0	23.8	88.0	385.9
Vacuum	Ag+  (3mol%)-RF2	82.4	24.4	141.2	567.7
Vacuum	Ag+  (1mol%)-RF2	82.3	21.8	101.3	485.1
Vacuum	Ag+  (1mol%)-RF2	81.1	23.7	138.3	689.4

200-816 nm.

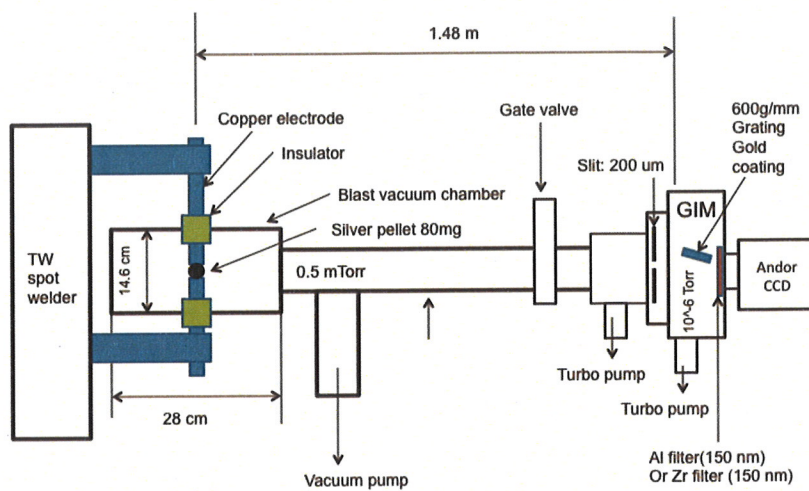
Figures 1A-C. Schematics of the light source comprising hydrated silver shot ignited with a spot welder, the intensity reducing, evacuated light conduit, and each of the three spectrometers to cover the spectral wavelength range of 10 nm to 816 nm. (A) Ultraviolet-visible (UV-Vis) spectrometer. (B) Normal incidence EUV spectrometer (NIS). (C) Grazing incidence EUV spectrometer (GIS).



(A)

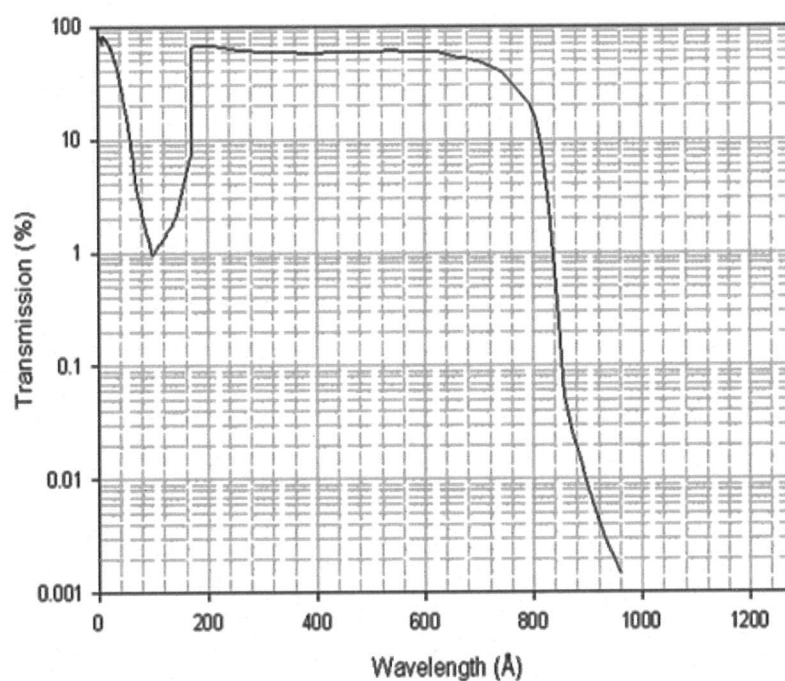


(B)

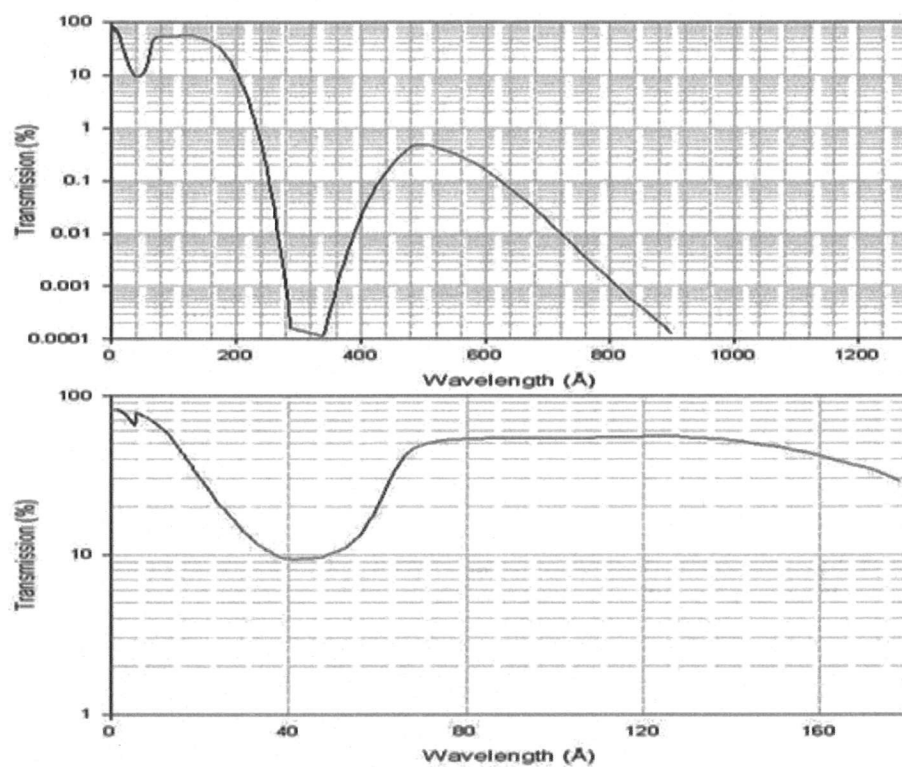


(C)

Figures 2A-B. Transmission curves of filters for EUV light that blocked visible light. (A) The Al filter (150 nm thickness) having a cutoff to short wavelengths at ~ 17 nm. (B) The Zr filter (150 nm thickness) having high transmission at the predicted H(1/4) transition cutoff 10.1 nm.



(A)



(B)

Figure 3. The efficiency of the Au 600 g/mm grating that was used to correct the GIS raw spectrum.

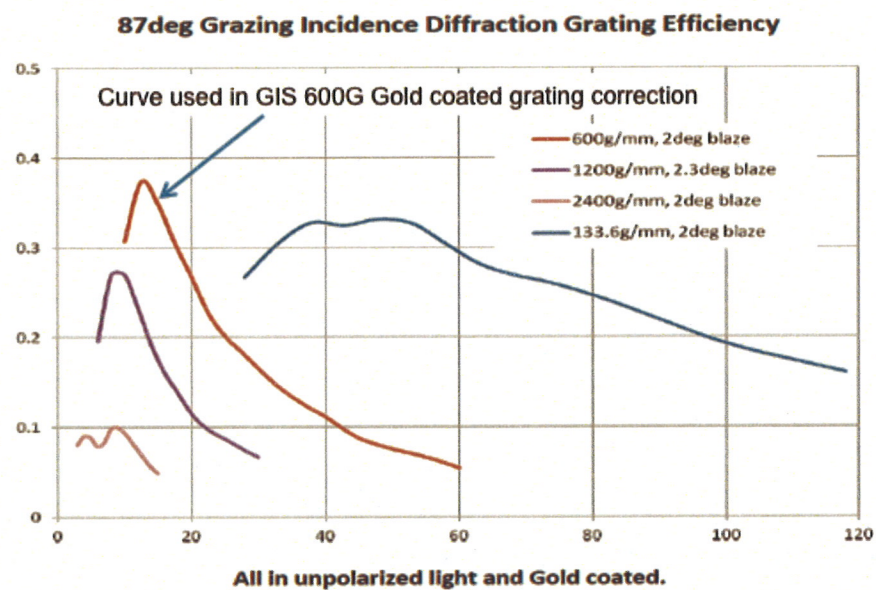


Figure 4. The EUV spectrum (5-50 nm) recorded with the GIS on a high voltage discharge of air that was used for wavelength calibration using the positions of known oxygen and ions.

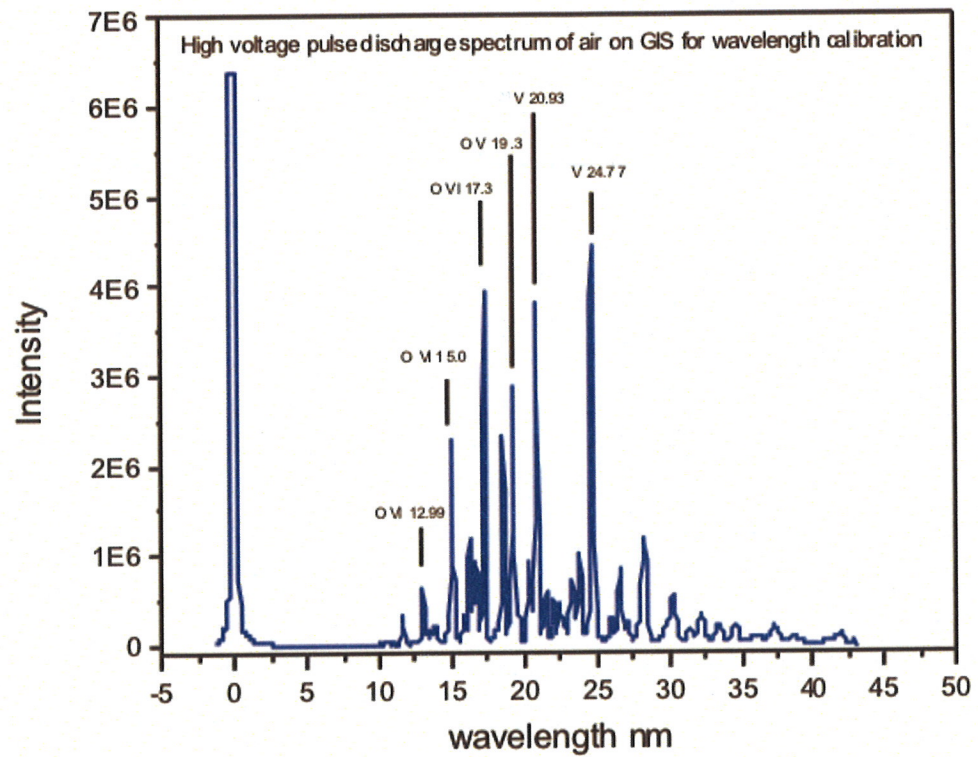


Figure 5. Transmission curve of the MgF_2 window that was used to correct the raw spectra acquired with the window.

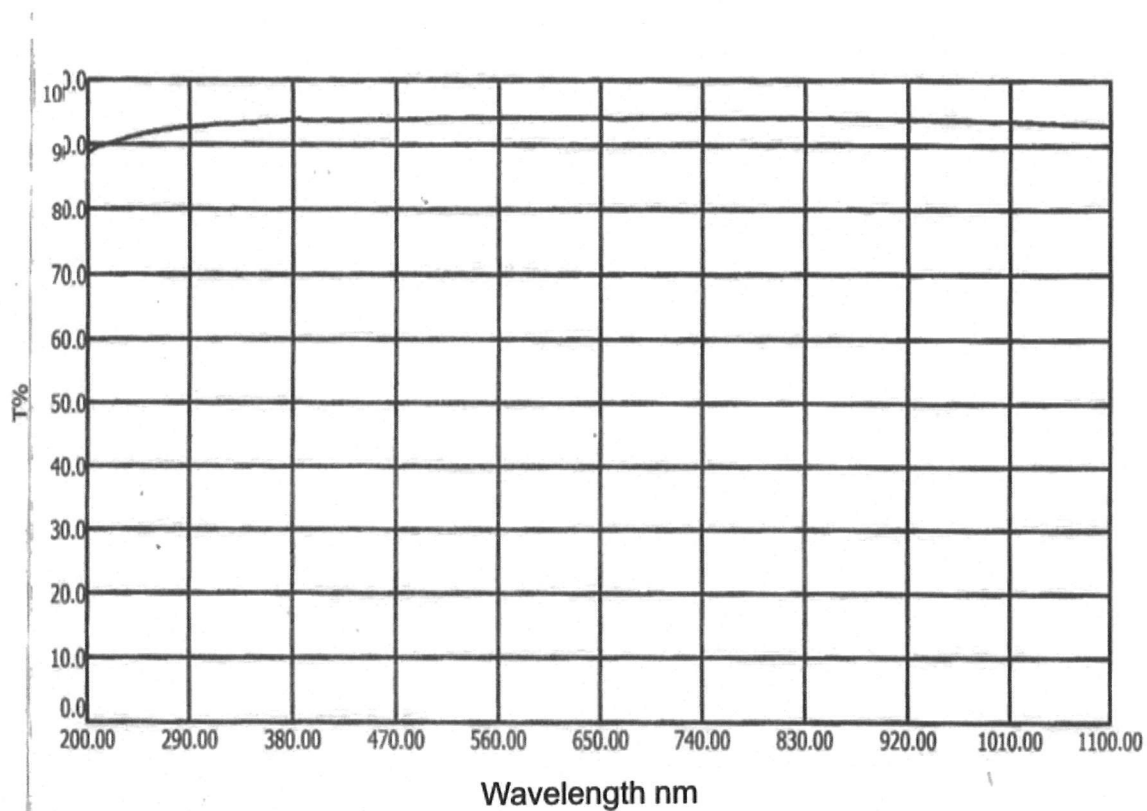


Figure 6. The reflectance and the efficiency of the Al-MgF₂ coated 300 g/mm grating. The NIS spectrum was only corrected by the reflectance since the efficiency was not well characterized.

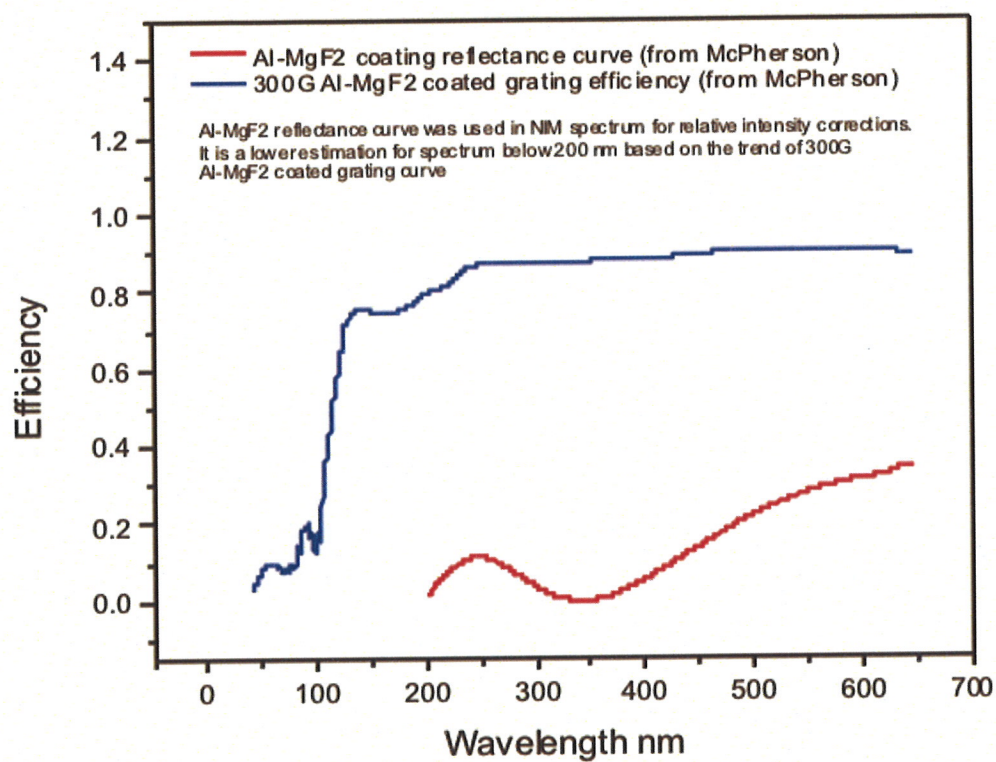


Figure 7. The CCD quantum efficiency that was used to correct the GIS and NIS raw spectra.

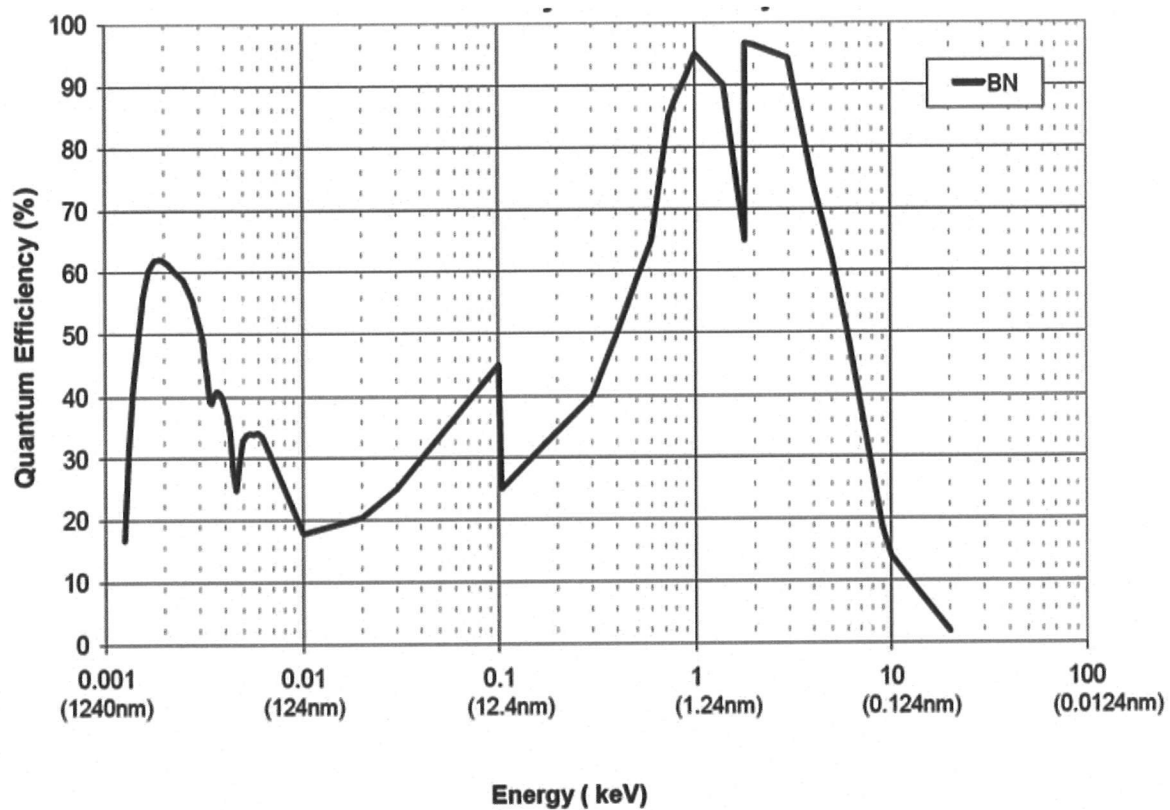


Figure 8. The raw spectra obtained using the GIS and NIS spectrometer to be processed with window, filter, grating, and CCD quantum efficiency corrections.

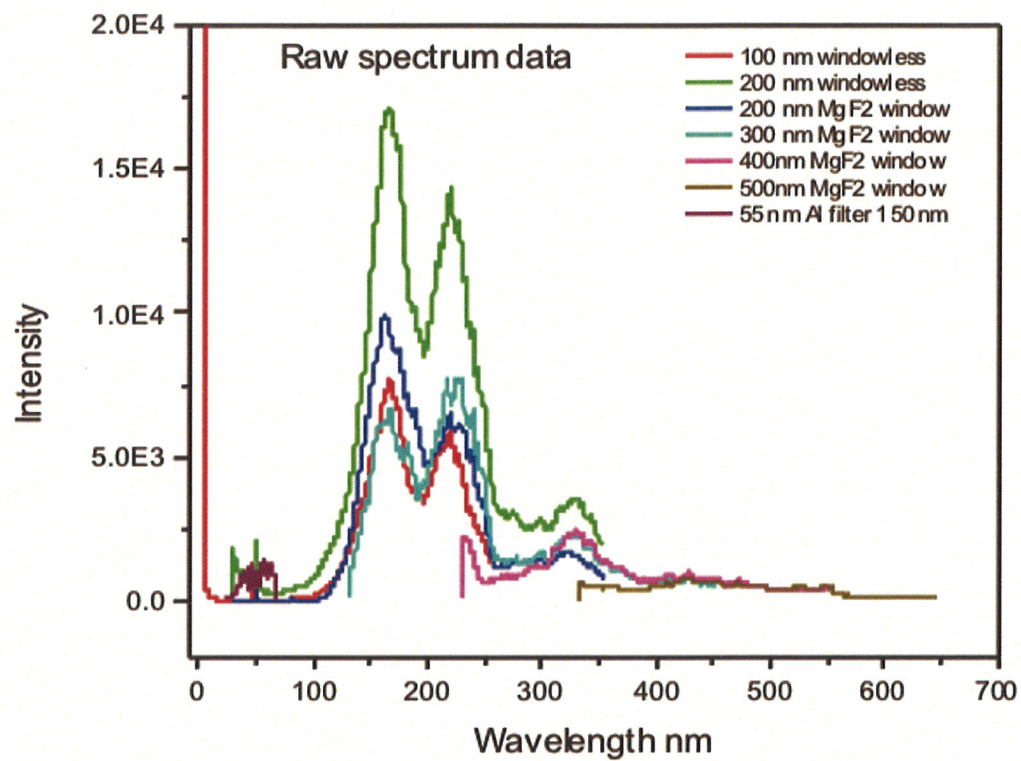


Figure 9. The combined GIS and NIS spectra following filter, grating, and CCD quantum efficiency corrections.

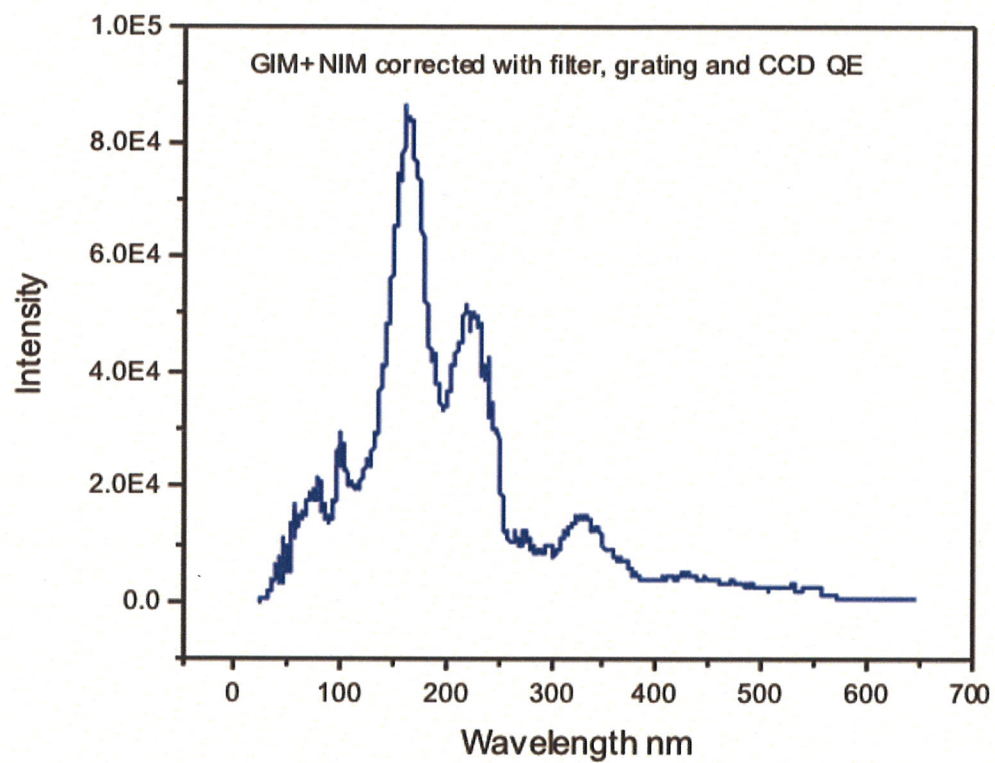


Figure 10. The combined GIS and NIS spectra before power calibration against the absolutely calibrated UV-Vis spectrum wherein the spectral count intensity of Figure 9 was converted to energy density by multiplying the counts as a function of wavelength by the conversion factor $\frac{hc}{\lambda}$.

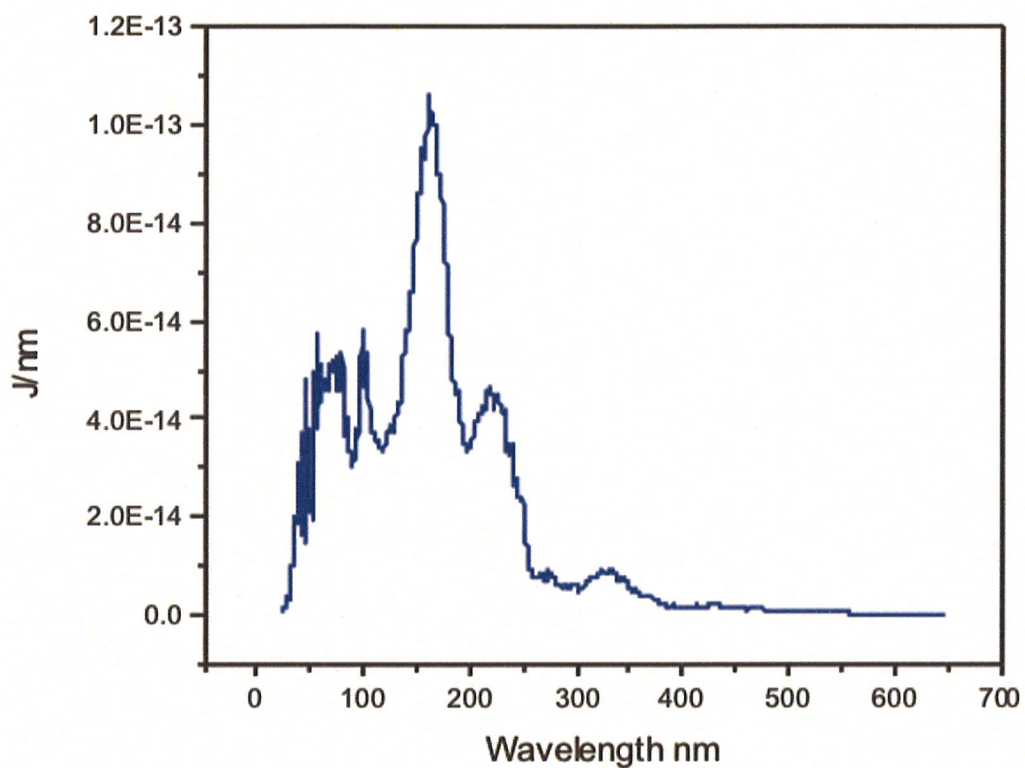


Figure 11. The wavelength calibrated and absolute intensity calibrated spectrum (22.8-647 nm) of the emission of hydrated silver shots comprising a source of H and HOH hydrino catalyst that were ignited by passing a low voltage, high current through the shot. The radiation is predominantly in the high-energy region with the predicted short wavelength emission of the H(1/4) continuum radiation.

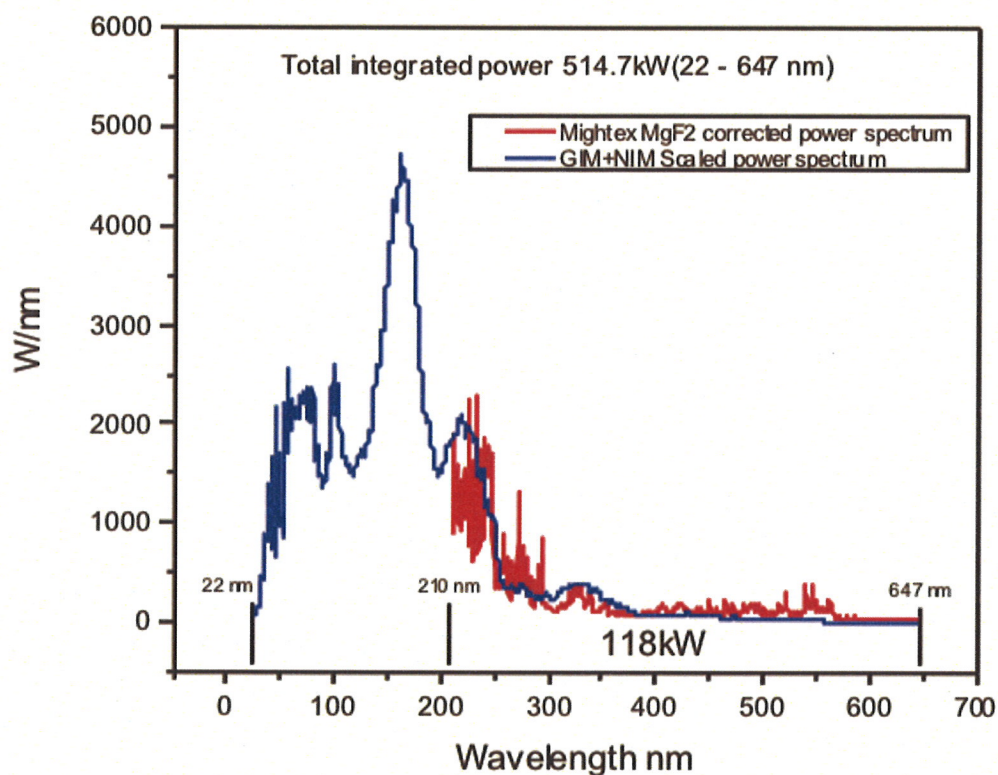


Figure 12. The wavelength calibrated and absolute intensity calibrated spectrum (10-480 nm) of the emission of hydrated silver shots taken with a new grating. The radiation is predominantly in the high-energy region with the predicted short wavelength emission of the H(1/4) continuum radiation and the short-wavelength H(1/4) cutoff is observed at 10.1 nm.

